Eur. Phys. J. C 51, 659–676 (2007)
DOI 10.1140/epjc/s10052-007-0328-1

THE EUROPEAN PHYSICAL JOURNAL C

Regular Article – Theoretical Physics

Proton–proton interaction in constituent quarks model at LHC energies

S. Bondarenko[1,a], E. Levin[2]

[1] II Theory Institute, Hamburg University, Luruper Chaussée 149, 22761, Hamburg, Germany
[2] HEP Department, School of Physics and Astronomy, Raymond and Beverly Sackler Faculty of Exact Science, Tel-Aviv University, Ramat Aviv, 69978, Israel

Received: 8 February 2006 / Revised version: 30 January 2007 /
Published online: 14 June 2007 – © Springer-Verlag / Società Italiana di Fisica 2007

Abstract. In this paper we consider soft processes at LHC energies in the framework of the constituent quark model. We show that this rather naive model is able to describe all available soft process data at lower energies and to predict the behavior of the total cross section, the elastic and diffractive cross sections at LHC energy. It turns out that the "input" pomeron that has been used in this approach has parameters that are close to the so called "hard" pomeron with rather large intercept $\Delta \approx 0.12$ and small value of the slope $\alpha'_P \approx 0.08\ \mathrm{GeV}^{-2}$. We show that the elastic amplitude has a minimum at impact parameter $b = 0$ and a maximum at $b \approx 2\ \mathrm{GeV}^{-1}$. Such a behavior is the result of overlapping of the parton clouds that belong to the different quarks in the hadron.

1 Introduction

One of the most challenging problems of QCD is to find the correct degrees of freedom for high energy "soft" interactions. The question is what set of quantum numbers diagonalizes the interaction matrix at high energies. The constituent quark model (CQM) [1, 2] is one of the models that may be a good candidate for a correct description of the "soft" interactions [3, 4]. In this model the constituent quarks play the roles of the correct degrees of freedom for high energy QCD and the structure of a hadron is characterized by two radii: the proper size of the constituent quark (R_Q) and the typical distance between two constituent quarks in a hadron (R). The main assumption is that $R \gg R_Q$.

In spite of the fact that this model looks rather naive, it is supported by the two sets of experimental data, namely, the CDF double parton cross section at the Tevatron, [5], and HERA data on inclusive diffraction production with nucleon excitation [6–10]. In our paper [11] we examined these data and found that the CQM model describes a lot of "soft" data in the first approximation; see also [12–15]. The radius of the constituent quark, which was found in [11], turned out to be small: $R^2_{\mathrm{quark}} \approx 0.1$–$0.2\ \mathrm{GeV}^{-2}$. However, this radius depends on energy (at least logarithmically as $R = R^2_{\mathrm{quark}} + 4\alpha_P \ln(W/W_0)$), and a possible scenario is that at the LHC energy this radius becomes compatible with the distance between the constituent quarks (R) (see Fig. 1). Therefore we could expect new physics at the LHC in such a scenario.

In this paper we are going to develop a systematic approach to high energy scattering in CQM. To our surprise we found that only the simplest diagrams of this model have been discussed in detail, namely the diagrams that include only the interaction between a pair of quarks. In our model we include all possible quark interactions, considering an eikonal approximation for the scattering amplitude of two colliding quarks (see Fig. 2). In this case, the first contribution to the elastic amplitude will simply be nine interactions between the constituent quarks in the protons. Further contributions to the amplitude will include the other interaction between the quarks (see Fig. 3). Taking into account all possible configurations of the quarks, we will obtain the amplitude that contains nine different contributions with alternating signs. Such a structure of the answer is similar to the scattering amplitude of light nuclei (tritium–tritium scattering). We will show that the

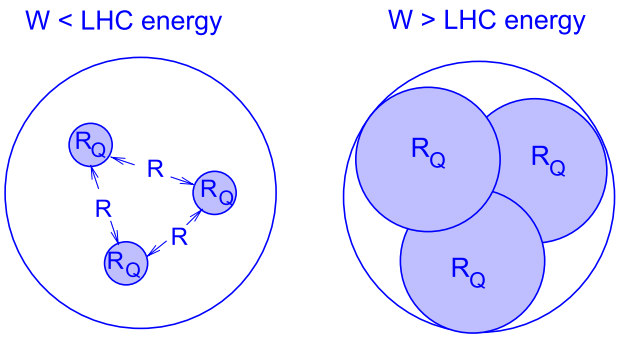

Fig. 1. The proton structure at different energies in CQM

[a] e-mail: sergb@mail.desy.de

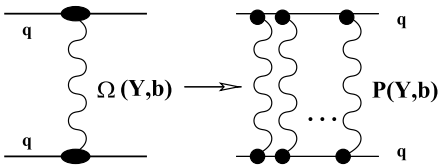

Fig. 2. The pomeron exchange and eikonalized quark–quark amplitudes

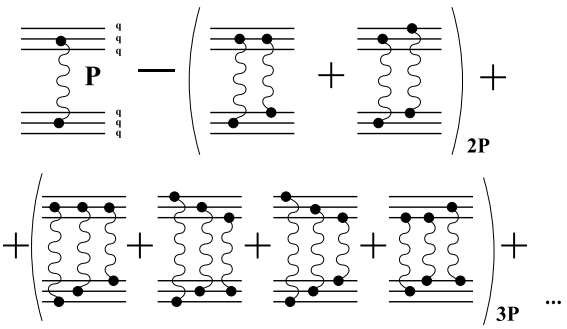

Fig. 3. The three first orders of the p–p elastic amplitude in the CQM

result satisfies the unitarity constraint, when we consider interactions between different configurations of the constituent quarks. The effects of the interaction of several pairs of quarks is especially important at high energies. If we consider our amplitude asymptotically at very high energy, where we may replace the eikonalized amplitude by a step function, the different parts of the amplitude will cancel each other, and only the last diagram, in which all quarks of the projectile interact with all quarks of the target, will survive. This last diagram will give a unitarized Froissart-like answer. In our estimates, it turns out that already at an energy of $\sqrt{s} = 1855\,\text{GeV}$ we need to consider the interaction of five pairs of quarks in the protons. At the LHC energies, the interaction of seven quark pairs is essential. This structure of the interaction changes not only the high energy dependence of the scattering amplitude, but it also leads to a quite different impact parameter dependence of the answer. In the case of these multi-pomeron exchanges between the different pairs of quarks, the amplitude has a minimum at low b. Such a change is very important, since it could affect the behavior of the slope both as a function of energy and as a function of momentum transfer.

Another interesting problem, addressed in this paper, is the values of the parameters of the "initial" pomeron. Indeed, it is widely believed that the "soft" pomeron has as its origin non-perturbative QCD contributions, which are out of theoretical control at the moment. Everything that we know about the "soft" pomeron is a mixture of our phenomenological knowledge with the general theoretical ideas on the properties of non-perturbative QCD contributions [16–27]. The question is the following: can we obtain the well known phenomenological pomeron using the "initial" pomeron with large intercept and small slope, i.e. the so called "hard" pomeron [28]? Does the "hard" pomeron play any role in the "soft" interactions? There exist two different points of view on this question. The first one is that we need to introduce separately two objects, "soft" and "hard" pomerons, which have different properties and contribute differently, each in a different kinematic region; see for example [16, 17, 20, 23] and references therein. Another point of view, see for example [29], is that non-perturbative physics enters our calculations only in the form of boundary and/or initial conditions and the "soft" pomeron arises as a result of unitarization effects and self-interactions of the "hard" pomerons in the amplitude. Our model may help to clarify this situation. Taking into account all effects of unitarization, eikonalization and accounting all interactions between the different configurations of the quarks, we will fit the experimental data. The fit will determine the parameters of the "initial" pomeron, such as its intercept and slope, as well as the radius of the constituent quark. We show in this paper that the parameters of the initial "soft" pomeron are close to the parameters of the "hard" pomeron and quite different from the parameters of the Donnachie–Landshoff pomeron [30, 31], which is usually considered as a typical "soft" pomeron.

The structure of the paper is as follows. In Sect. 2 we discuss in more detail our approach and methods of calculation. In Sect. 3 we apply our model to the p–p data and fit the experimental data in order to find numerical values of the parameters of the "initial" pomeron. Section 4 is dedicated to the elastic amplitude as a function of the impact parameter. In this section we also consider the different contributions to the elastic amplitude due to interactions of different numbers of quark–quark pairs. In Sect. 5 we calculate the survival probability (SP) of the exclusive hard processes in p–p scattering. The cross section of the diffractive dissociation process is calculated in Sect. 6. The last section, our conclusion, contains the main results of the paper as well as a discussion of future work in the proposed direction.

2 Proton–proton scattering in the pomeron approach

The key ingredient of the CQM is the quark–quark scattering amplitude. Considering this model, we need to determine the form of single pomeron exchange between two quarks. The next step will be the eikonalization of the single scattering amplitude, which means a replacement of the single pomeron exchange in the scattering of the particular pair of quarks by the eikonal amplitude. The third step in our calculation will be the consideration of the interactions between all possible quark configurations in colliding protons (see Fig. 3). For this last step we need to know the wave function of the quarks in the proton and the vertices of the pomeron–quark interactions. Only after the determination of the wave function and vertices we will be able to calculate the diagrams for proton–proton scattering.

Now, let us consider these problems step by step.

2.1 Quark–quark interactions

We determine the amplitude for q–q and p–p scattering in the impact parameter representation. In this case the "soft" pomeron exchange for the interaction of the pair of quarks (pomeron propagator) has the following form (see for more on soft pomerons [21, 30–32]):

$$\Omega_{q-q}(Y,b) = \sigma_0 \mathrm{e}^{\Delta Y} \frac{\mathrm{e}^{-b^2/R^2}}{\pi R^2}\,; \tag{1}$$

here $Y = \ln(s/1\,\mathrm{GeV}^2)$ is the rapidity of the process, b is the impact parameter of the process, Δ is the intercept of the "initial", input pomeron, and

$$R^2 = 8R_Q^2 + 4\alpha'_P \ln(s/s_0)\,. \tag{2}$$

Here R_Q^2 is the squared radius of the constituent quark, and α'_P is the slope of the trajectory of the input pomeron. We will find the numerical values of σ_0, Δ, R_Q^2 and α'_P by fitting the data for p–p scattering. We determine the eikonal amplitude, which is a "major" ingredient in our calculations, as follows:

$$P_{q-q}(Y,b) = 1 - \mathrm{e}^{-\Omega_{q-q}(Y,b)/2}, \tag{3}$$

see Fig. 2, where P_{q-q} is the imaginary part of the quark–quark scattering amplitude at high energy. Below, discussing the single quark–quark interaction amplitude, we will mean only the amplitude given by (3). We will consider the pomeron of (1) only as the "input", initial pomeron of our problem.

2.2 The model of the proton

In order to take into account all possible configurations of the interacting pairs of quarks, see Fig. 3 and all figures in the appendices, we need to know the analytical expressions for the vertices of the quark–pomeron interactions. It is clear that we need to calculate only the three types of such vertices, see Figs. 4–6, in which there are one, two or three groups of pomerons attached to one, two or three quarks. In order to calculate these vertices we need to know the wave functions of the constituent quarks inside a proton. We use a very simple Gaussian model for this wave function, which corresponds to an oscillatory potential between a pair of quarks in a proton. In this model we have [33]

$$\Psi = \frac{\alpha}{\pi\sqrt{3}} \mathrm{e}^{-\frac{\alpha}{2}\left(\sum x_i^2\right)}, \tag{4}$$

where the constant α is related to the electromagnetic radius of the proton:

$$\alpha = 1/R^2_{\mathrm{electr}} \approx 0.06\,\mathrm{GeV}^2. \tag{5}$$

For the impact factor presented in Fig. 4, we have

$$V_1(q) = \int \prod_{i=1}^{3} \mathrm{d}x_i\, |\Psi(x_1,x_2,x_3)|^2 \delta(\mathbf{x}_1+\mathbf{x}_2+\mathbf{x}_3) \mathrm{e}^{\mathrm{i}\mathbf{q}\mathbf{x}_1} = \mathrm{e}^{-\frac{q^2}{6\alpha}}. \tag{6}$$

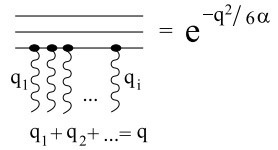

Fig. 4. The one pomeron vertex in quark–quark interaction

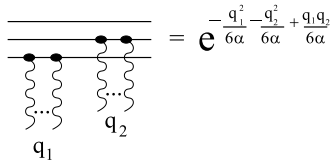

Fig. 5. Two pomeron vertex in quark–quark interaction

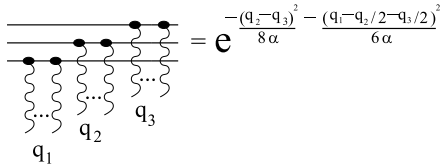

Fig. 6. The three Pomeron vertex in q–q interaction

The impact factor for two groups of pomerons attached to two different quarks is shown in Fig. 5:

$$V_2(q_1,q_2) = \int \prod_{i=1}^{3} \mathrm{d}x_i\, |\Psi(x_1,x_2,x_3)|^2 \delta(\mathbf{x}_1+\mathbf{x}_2+\mathbf{x}_3) \times \mathrm{e}^{\mathrm{i}\mathbf{q}_1\mathbf{x}_1+\mathbf{q}_2\mathbf{x}_2} = \mathrm{e}^{-\frac{q_1^2}{6\alpha}-\frac{q_2^2}{6\alpha}+\frac{\mathbf{q}_1\mathbf{q}_2}{6\alpha}}. \tag{7}$$

The last impact factor is the vertex of Fig. 6. We have for this vertex

$$V_3(q_1,q_2,q_3) = \int \prod_{i=1}^{3} \mathrm{d}x_i |\Psi(x_1,x_2,x_3)|^2 \delta(\mathbf{x}_1+\mathbf{x}_2+\mathbf{x}_3) \times \mathrm{e}^{\mathrm{i}\mathbf{q}_1\mathbf{x}_1+\mathbf{q}_2\mathbf{x}_2+\mathbf{q}_3\mathbf{x}_3} = \mathrm{e}^{-\frac{(\mathbf{q}_2-\mathbf{q}_3)^2}{8\alpha}-\frac{(\mathbf{q}_1-\mathbf{q}_2/2-\mathbf{q}_3/2)^2}{6\alpha}}. \tag{8}$$

In all three cases the total transferred momentum of the diagrams is defined as the sum of the transverse momenta of all pomerons (q_i): $k = \sum q_i$.

2.3 The elastic amplitude of p–p scattering

We have all ingredients for the calculation of the elastic amplitude. In the CQM we can write the imaginary part of the amplitude as the sum of the imaginary parts of the amplitudes that describe the interactions between different numbers of quark pairs:

$$\mathrm{Im}\,A(s,b) = \mathrm{Im}\,A_{1\mathrm{pair}}(s,b) - \mathrm{Im}\,A_{2\mathrm{pairs}}(s,b) + \mathrm{Im}\,A_{3\mathrm{pairs}}(s,b) + \ldots + \mathrm{Im}\,A_{9\mathrm{pairs}}(s,b)\,. \tag{9}$$

The maximum number of possible quark pair interactions in the amplitude is nine. The three first orders of the possible configurations of interactions are shown in Fig. 3 and the calculations of all other orders are presented in Appendix . The amplitude defined in a such way incorporates unitarity by construction. Indeed, checking the expressions for the different terms of the amplitude that are written in Appendix B, it is easy to see that at asymptotically high energies only the last term of (9) will survive, giving a Froissart-like answer for the whole amplitude.

We proceed to calculate the contribution of the first diagram of Fig. 3, i.e. the first term of the r.h.s. of (9). We perform a Fourier transformation of the vertex of (6) from momentum to impact parameter space:

$$\hat{V}_1(b) = \int \frac{\mathrm{d}^2q}{4\pi^2}\mathrm{e}^{-q^2/(6\alpha)+\mathrm{i}\mathbf{qb}} = \frac{3\alpha}{2\pi}\mathrm{e}^{-\frac{3\alpha}{2}b^2}. \tag{10}$$

Using this vertex we obtain the contribution to the elastic amplitude from the one pomeron exchange $A_{1q-q}(s,b)$, which is

$$\begin{aligned}\mathrm{Im}\, A_{1\mathrm{pair}}(s,b) = 9\frac{9\alpha^2}{4\pi^2}\int \mathrm{d}^2b_1 \int \mathrm{d}^2b_2\, \mathrm{e}^{-\frac{3\alpha}{2}(\mathbf{b}-\mathbf{b}_1)^2} \\ \times P_{q-q}(Y,b_2)\mathrm{e}^{-\frac{3\alpha}{2}(\mathbf{b}_1-\mathbf{b}_2)^2},\end{aligned} \tag{11}$$

where the first coefficient in (11) is the total number of q–q interactions in this order. Using more complicated vertices, which are given by (7) and (8), we calculate all terms that contribute to the elastic amplitude, i.e. terms at the r.h.s. of (9). In Appendices and the resulting expressions for the amplitude $A(s,b)$ are written, as well as examples are given of calculations of diagrams with different numbers of interacting pairs of quarks.

2.4 The total, elastic cross sections and the elastic slope B_{el} of the proton–proton interaction

The expression for the amplitude (Appendix B) is determined in the impact parameter space and now we can easily calculate the different cross sections for the processes of interest.

First, we consider σ_{tot}.

The total cross section in the impact parameter representation is simply

$$\sigma_{\mathrm{tot}}(s) = 2\int \mathrm{d}^2b\, \mathrm{Im}\, A(s,b)\,. \tag{12}$$

Fitting the experimental data at low energies we also add to this cross section the contribution of the secondary reggeons, $\sigma^{\mathrm{Reg}}_{\mathrm{tot}}$ [34].

Next, we consider σ_{el}.

The elastic cross section in the same framework is equal:

$$\sigma_{\mathrm{el}}(s) = \int \mathrm{d}^2b|A(s,b)|^2 = \int \mathrm{d}^2b(\mathrm{Im}\, A(s,b))^2. \tag{13}$$

where we treat the quark–quark amplitude as mostly imaginary, as is usually assumed for the pomeron.

Finally, we consider B_{el}.

We consider only the first term of the elastic amplitude, i.e. $A_{1q-q}(s,b)$. In this case we have for the forward ($t=0$) elastic exponential slope B_{el}:

$$\begin{aligned}B_{\mathrm{el}} = \frac{9\alpha^2}{4\pi^2}\int \mathrm{d}^2b_1 \int \mathrm{d}^2b_2 \int \mathrm{d}^2b\, b^2\mathrm{e}^{-\frac{3\alpha}{2}(\mathbf{b}-\mathbf{b}_1)^2} \\ \times P_{q-q}(Y,b_2)\mathrm{e}^{-\frac{3\alpha}{2}(\mathbf{b}_1-\mathbf{b}_2)^2} \\ \Big/ 2\int \mathrm{d}^2bP_{q-q}(Y,b) \\ = \frac{1}{\alpha}\frac{\sigma^{1q-q}_{\mathrm{tot}}}{\sigma^{1q-q}_{\mathrm{tot}}} + \frac{\int \mathrm{d}^2b\, b^2P_{q-q}(Y,b)}{\sigma^{1q-q}_{\mathrm{tot}}}\,.\end{aligned} \tag{14}$$

Here

$$\sigma^{1q-q}_{\mathrm{tot}} = 2\int \mathrm{d}^2b\, P_{q-q}(Y,b)\,.$$

We add the contribution of the secondary reggeons to this expression, which one needs to take into account at low energies:

$$\begin{aligned}B_{\mathrm{el}} = \frac{9\sigma^{1q-q}_{\mathrm{tot}}}{9\sigma^{1q-q}_{\mathrm{tot}}+\sigma^{\mathrm{Reg}}_{\mathrm{tot}}}R^2_{\mathrm{electr}} + \frac{9\int \mathrm{d}^2b\, b^2P_{q-q}(Y,b)}{9\sigma^{1q-q}_{\mathrm{tot}}+\sigma^{\mathrm{Reg}}_{\mathrm{tot}}} \\ + 2\big(\alpha'_R-\alpha'_{\mathrm{SP}}\big)\ln(s/s_0)\frac{\sigma^{\mathrm{Reg}}_{\mathrm{tot}}}{9\sigma^{1q-q}_{\mathrm{tot}}+\sigma^{\mathrm{Reg}}_{\mathrm{tot}}}\,.\end{aligned} \tag{15}$$

The third term of the r.h.s. of (15) contains the contribution of the secondary reggeons, which we do not consider in our model. We take the secondary reggeons into account only on the level of proton–proton scattering. Therefore, the parameters that we take for this contribution have a pure phenomenological origin. We take for the slope of the secondary reggeons $\alpha'_{\mathrm{R}} = 0.86\,\mathrm{GeV}^{-2}$ and for the slope of the phenomenological "soft" pomeron[1] $\alpha'_{\mathrm{SP}} = 0.25\,\mathrm{GeV}^{-2}$ at $\sqrt{s_0} = 9\,\mathrm{GeV}$ in the r.h.s. of (15) [30–32, 34]. Generalizing this expression to the case of the full elastic amplitude (see (9)) at low energies we obtain

$$\begin{aligned}B_{\mathrm{el}} = \frac{9\sigma^{1q-q}_{\mathrm{tot}}}{\sigma_{\mathrm{tot}}+\sigma^{\mathrm{Reg}}_{\mathrm{tot}}}R^2_{\mathrm{electr}} + \frac{9\int \mathrm{d}^2b\, b^2P_{q-q}(Y,b)}{\sigma_{\mathrm{tot}}+\sigma^{\mathrm{Reg}}_{\mathrm{tot}}} \\ + 2\big(\alpha'_{\mathrm{R}}-\alpha'_{\mathrm{SP}}\big)\ln(s/s_0)\frac{\sigma^{\mathrm{Reg}}_{\mathrm{tot}}}{\sigma_{\mathrm{tot}}+\sigma^{\mathrm{Reg}}_{\mathrm{tot}}} \\ + \sum_{i=2}^{9}\frac{\int \mathrm{d}^2b\, b^2\,\mathrm{Im}\, A_i(b,s)}{\sigma_{\mathrm{tot}}+\sigma^{\mathrm{Reg}}_{\mathrm{tot}}}\,,\end{aligned} \tag{16}$$

[1] The slope α'_{SP} is the slope of the phenomenological pomeron in proton–proton scattering [30–32, 34], and it is not related to the slope α'_P of our "initial" pomeron in quark–quark scattering.

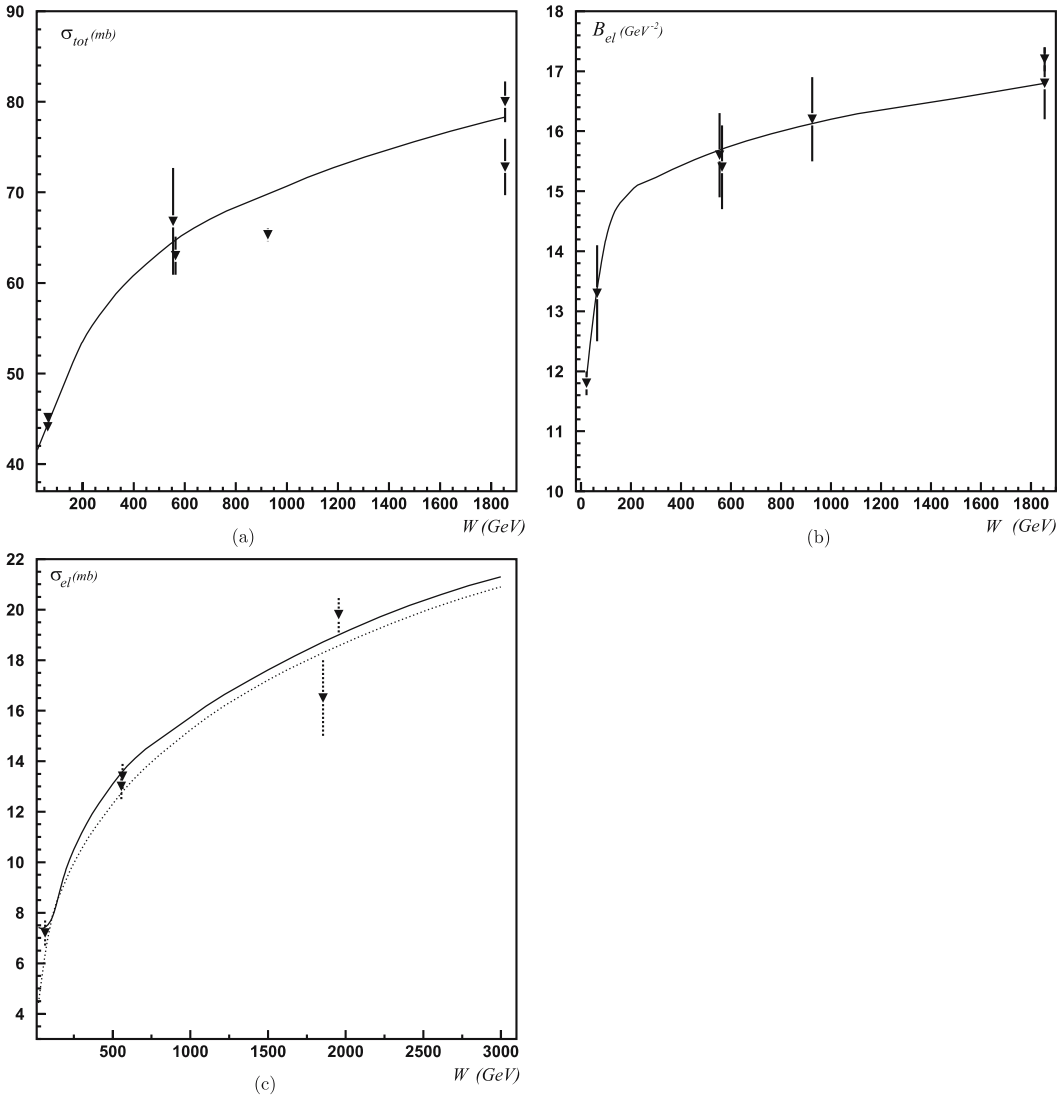

Fig. 7. The plots for the total cross section (**a**), elastic cross section (**c**), and elastic slope (**b**). The experimental data are from [34] and references therein

whereas at high energy we have

$$B_{\rm el} = \frac{9\sigma_{\rm tot}^{1q-q}}{\sigma_{\rm tot}} R^2_{\rm electr} + \frac{9\int {\rm d}^2b\, b^2 P_{q-q}(Y,b)}{\sigma_{\rm tot}} + \sum_{i=2}^{9} \frac{\int {\rm d}^2b\, b^2\, {\rm Im}\, A_i(b,s)}{\sigma_{\rm tot}}\,. \tag{17}$$

It is also interesting to calculate the elastic cross section using the simple expression for the elastic cross section that is obtained in the model with the phenomenological "soft" pomeron. Indeed, in this case we calculate the elastic cross section using the following formula:

$$\sigma_{\rm el}(s) = \frac{\sigma^2_{\rm tot}}{16\pi B_{\rm el}}\,. \tag{18}$$

This expression is correct only in the case when one "soft" pomeron is considered. It will be interesting to compare the calculations of the elastic cross section given by (13) with the calculations of (18). Indeed, in this case we check the possibility that one may reproduce the simple result of (18) by the theory in which many eikonalized pomeron exchanges are taken into account. So, in the next section we will perform data fitting and will make the calculations using both expressions, (13) and (18), in order to show the importance of interaction of many quark pairs.

3 The proton–proton scattering data and the parameters of the input pomeron

Now we are able to apply our model to the p–p interactions and, fitting the experimental observables, we will extract the values of the parameters of our input pomeron (see (1)). In Fig. 7 we present the plots for the total cross section, the elastic cross section and the elastic slope in the energy range $W = 23$–$1855\,{\rm GeV}$. We perform all calculations numerically[2] using the formulae of the previous subsection with the amplitude written in Appendix B. There

[2] The Fortran code can be obtained by e-mail request; sergb@mail.desy.de.

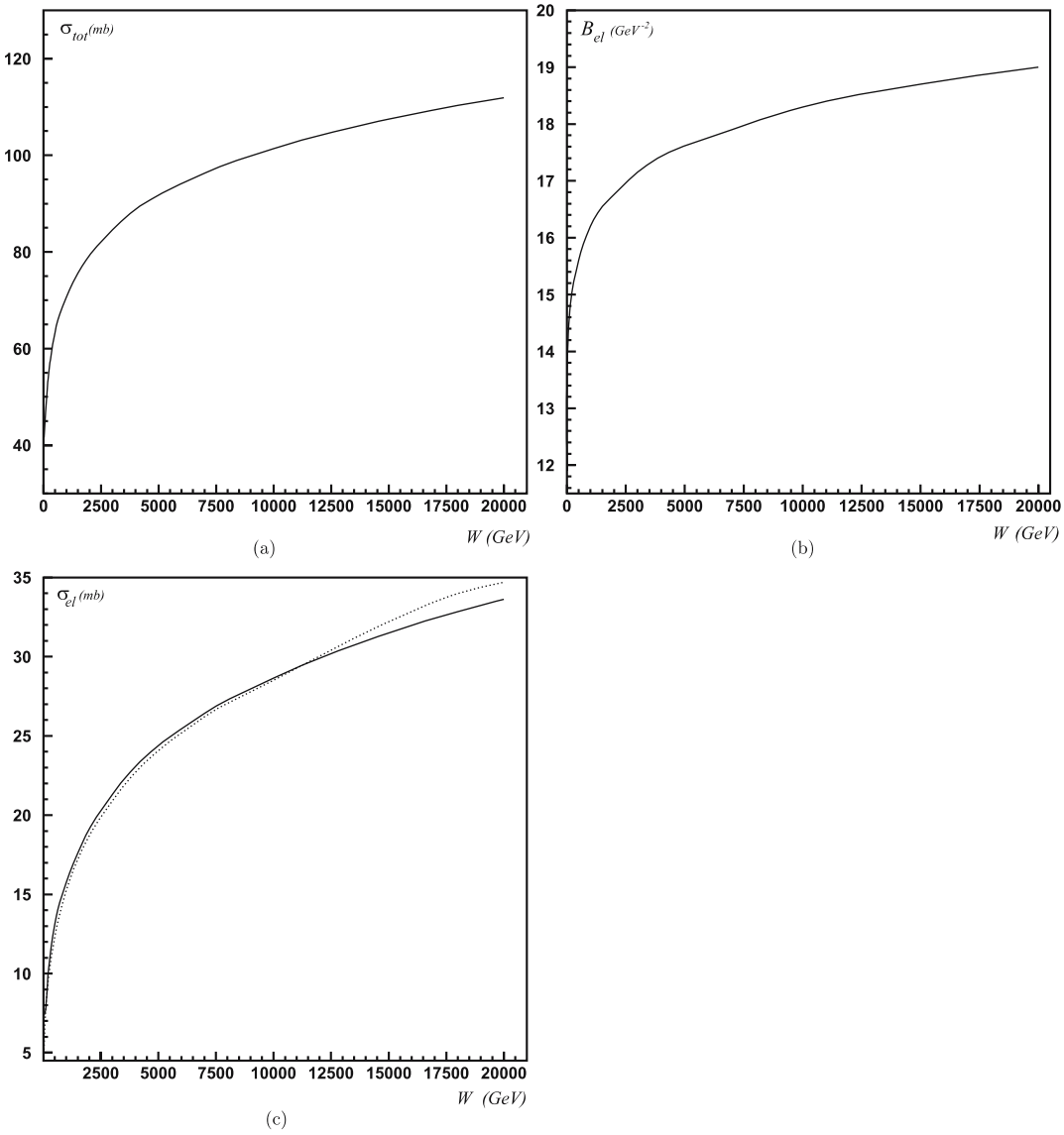

Fig. 8. The plots for the total cross section (**a**), elastic cross section (**c**), and elastic slope (**b**), at high energies

are two different plots that we present for the elastic cross section using definitions (13) and (18). The solid line represents the elastic cross section given by (18), and the dashed line represents calculations performed with (13).

From these plots we see that the model describes the experimental data quite well. The parameters of the single pomeron of (1) extracted from the data fitting are the following:

- the slope of the input pomeron trajectory:

$$\alpha' = 0.08\,\mathrm{GeV}^{-2}\,; \tag{19}$$

- the input pomeron's intercept:

$$\Delta = 0.118\,; \tag{20}$$

- the value of the cross section for the input pomeron at $s_0 = 1\,\mathrm{GeV}^2$:

$$\sigma_0 = 6.3\,\mathrm{GeV}^{-2}\,; \tag{21}$$

- the radius of the constituent quark:

$$R^2_{\mathrm{quark}} = 0.16\,\mathrm{GeV}^{-2}\,. \tag{22}$$

With these parameters we extrapolate our calculations for the cross sections and slope at higher energies. The resulting plots are shown in Fig. 8.

It should be stressed that the above parameters are quite different from the Donnachie–Landshoff pomeron [30, 31]. The pomeron intercept that we obtained is higher and the slope is much lower than the intercept and the slope of the D–L pomeron. We may conclude that such a small value of the pomeron slope indicates that our input pomeron may have a "hard" origin.

4 Behavior of the elastic amplitude of p–p scattering in our model

The elastic amplitude in our model has a sufficiently complex structure. It contains contributions from different con-

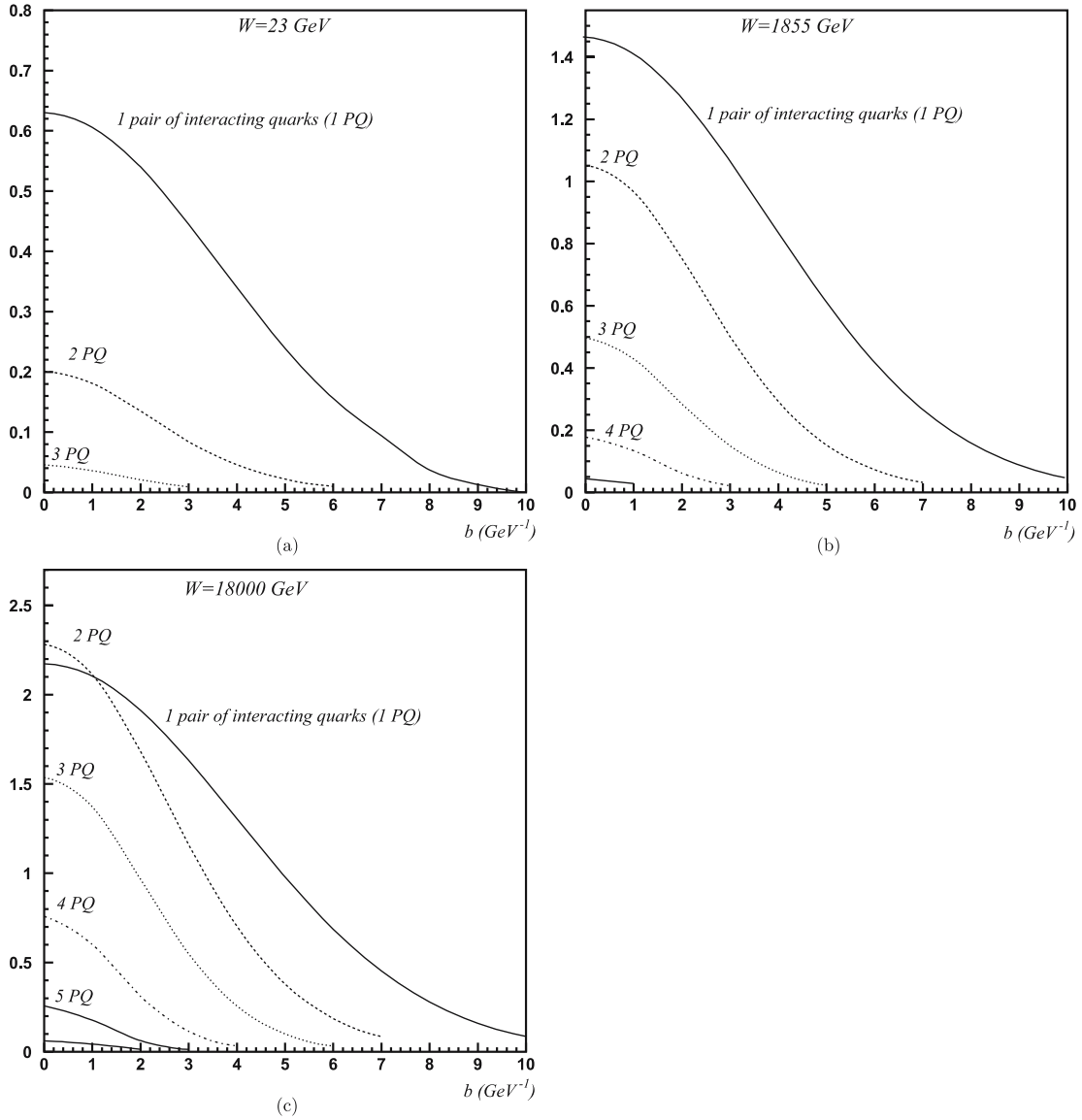

Fig. 9. The contributions to the elastic amplitude from the interactions of different numbers of quark pairs at different energies

figurations for the interactions of the quarks inside the protons. We found all possible terms that contribute to the elastic amplitude, see Appendix B, and, therefore, we can find which terms in the elastic amplitude are important at different energies. It turns out that even at low energies the interactions of two quark pairs, i.e. the interactions between two quarks in one proton with two quarks in another proton, are not negligible. At Tevatron energy, $\sqrt{s} = 1855\,\text{GeV}$, we already need to take into account the contributions from five pairs of interacting quarks. At energy of the order of the LHC energy, $\sqrt{s} = 15\,000\,\text{GeV}$, the contribution of the interaction of seven quark pairs is significant. At this energy the contribution of two quark pair interaction exceeds the contribution of one quark pair interaction (see Fig. 9). This is a signal that the parton clouds start to overlap, leading to the picture of Fig. 1.

From Fig. 9 we also see that even at energy $\sqrt{s} = 1855\,\text{GeV}$, the one quark pair contribution to the elastic amplitude exceeds unity. The unitarization of the amplitude in this case is achieved not by eikonalization of the quark–quark interaction, but by including more complicated configurations of the quarks inside the protons in the elastic amplitude. Therefore, the form of the impact parameter dependence of the amplitude turns out to be different from the usual Gaussian one. Indeed, the contribution of two quark pair interactions, which have a negative sign in the amplitude, is equal to or larger than the contribution of one quark pair interaction. At the same time the one quark pair interaction is wider in the impact parameter space (see again Fig. 9). The contributions of all terms in the elastic amplitude lead, therefore, to a situation in which the maximum of the elastic amplitude moves from zero impact parameter to the impact parameter $b \approx 2\,\text{GeV}^{-1}$ (see Fig. 10). This effect reflects very simple physics. At high energy at small impact parameter the multiple quark pair interactions are important and elastic production becomes mostly peripheral.

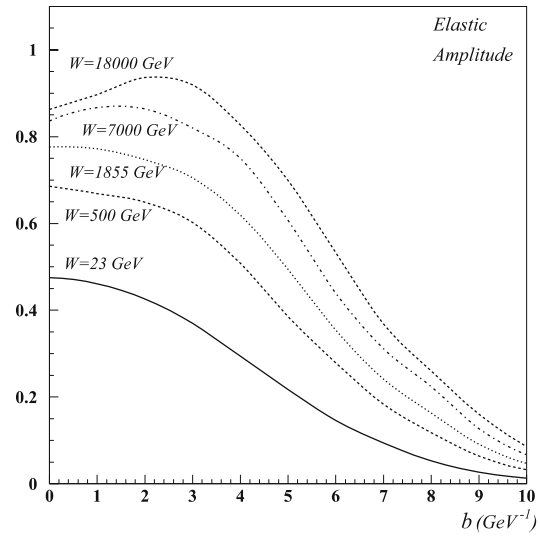

Fig. 10. The elastic amplitude of the p–p scattering as a function of impact parameter at different energies

5 Survival probability of the "hard" processes in p–p scattering

In this section we consider the calculation of the survival probability for the process $p+p \to p+[\mathrm{LRG}]+\mathrm{dijet}+[\mathrm{LRG}]+p$, where p and p are the colliding protons and LRG is the large rapidity gap. In this process there are two large rapidity gaps – the rapidity intervals without secondary hadrons. The cross sections of such processes are small in comparison with the inclusive production, or, in other words, in comparison with the process in which no rapidity gap is selected. We call the ratio of these two processes, exclusive and inclusive (or the process without LRG), the survival probability of the large rapidity gap [35, 36]. In the simple case of the eikonal approach to the proton–proton interaction, the survival probability is determined by a simple formula [35–38]:

$$\hat{S}^2 = \frac{\int \mathrm{d}^2b\, A(s,b)\sigma_{\mathrm{hard}}(b)}{\int \mathrm{d}^2\, b\sigma_{\mathrm{hard}}(b)}\,, \tag{23}$$

where

$$A(s,b) = \mathrm{e}^{-\Omega(s,b)} \tag{24}$$

is the probability that no inelastic interaction between the scattered hadrons has occurred at energy $\sqrt{s}$ and impact parameter b.

Using a simple Gaussian parameterization for $\sigma_{\mathrm{hard}}(b)$, namely

$$\sigma_{\mathrm{hard}}(b) = \sigma_{\mathrm{hard}}\frac{\mathrm{e}^{-\frac{b^2}{R^2_{\mathrm{H}}}}}{4\pi R^2_{\mathrm{H}}}\,, \tag{25}$$

with the following value of the radius R^2_{H} estimated in [37, 38] on the base of the HERA data [39], for the elastic J/ψ photoproduction:

$$R^2_{\mathrm{H}} = 8\,\mathrm{GeV}^{-2}, \tag{26}$$

we reduce (23) to the form

$$\hat{S}^2 = \frac{1}{\pi R^2_{\mathrm{H}}}\int \mathrm{d}^2b\, A(s,b)\mathrm{e}^{-\frac{b^2}{R^2_{\mathrm{H}}}}. \tag{27}$$

The difference of the calculation of the SP in our model from the calculations above is that we consider as principal degrees of freedom the constituent quarks, but not the protons. Therefore, we need to determine the expression for SP in terms of the interacting quark pairs. We begin with the discussion of the cross section for the exclusive "hard" production in the case of interaction of only one pair of quarks. For this process we have

$$\sigma_{\mathrm{hard}}(b) = \sigma_{\mathrm{hard}}\big(\hat{A}_{1\mathrm{pair}}(s,b)\big)^2, \tag{28}$$

with the amplitude $\hat{A}_{1\mathrm{pair}}(s,b)$, calculated from (11) with the following replacement:

$$P_{q-q}(Y,b_2) \to \frac{\mathrm{e}^{-\frac{b_2^2}{2R^2_{Q-H}}}}{2\pi R^2_{\mathrm{H}}}\hat{P}_{q-q}(Y,b_2)\,, \tag{29}$$

where

$$\hat{P}_{q-q}(Y,b_2) = 1 - P_{q-q}(Y,b_2) = \mathrm{e}^{-\Omega_{q-q}(Y,b_2)/2} \tag{30}$$

in (29) means that no inelastic interactions occur between the pair of quarks considered. This pair of quarks, which produces a "hard" jet, interacts elastically. The amplitude of this process is illustrated in Fig. 11. In the expression for $\hat{A}(s,b)$, we need to introduce a new "hard" radius $R^2_{Q\mathrm{H}}$, which is related to the "hard" process on the quark level. We find the numerical value of $R^2_{Q\mathrm{H}}$ in the following way. For the simplest process of "hard" production without any "soft" rescattering, the answer will be the same for any model:

$$\mathrm{e}^{-\frac{b^2}{2R^2_{\mathrm{H}}}} = 9\frac{9\alpha^2}{4\pi^2}\int \mathrm{d}^2b_1\int \mathrm{d}^2b_2\,\mathrm{e}^{-\frac{3\alpha}{2}(\mathbf{b}-\mathbf{b}_1)^2} \times \mathrm{e}^{-\frac{b_2^2}{2R^2_{Q\mathrm{H}}}}\mathrm{e}^{-\frac{3\alpha}{2}(\mathbf{b}_1-\mathbf{b}_2)^2}. \tag{31}$$

Indeed, we can see that, using this equality in (28), we reproduce the expression given by (25). From (31) we obtain the value of $R^2_{Q\mathrm{H}}$:

$$R^2_{Q\mathrm{H}} \approx 1.1\,\mathrm{GeV}^{-2}. \tag{32}$$

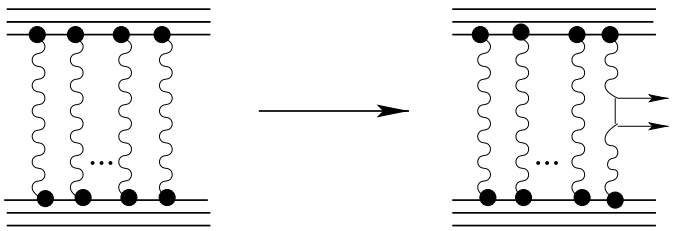

Fig. 11. The first order amplitude of the LRG "hard" process

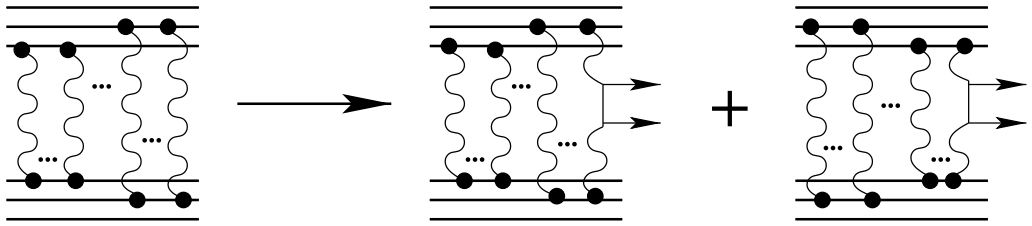

Fig. 12. The general structure of the amplitude of the LRG "hard" process for the case of interaction of two quark pairs

Table 1. The survival probability factor as a function of $\sqrt{s}$

$SP(\sqrt{s} = 23\ \text{GeV})$	$SP(\sqrt{s} = 1855\ \text{GeV})$	$SP(\sqrt{s} = 15\,000\ \text{GeV})$	$SP(\sqrt{s} = 18\,000\ \text{GeV})$
0.23	0.052	0.0175	0.0155

Generalizing the procedure defined by (29) we obtain the answer for the SP amplitude, $\hat{A}(s,b)$, in all orders. Indeed, any term of the amplitude given in Appendix B, see (B.1), has an integration over the product of eikonalized amplitudes of interacting quark pairs, $P_{q-q}(b_i)\dots P_{q-q}(b_j)$. When we calculate the SP, we should take into account the possibility that the "hard" process can occur in the interaction of any pair of quarks. Therefore, for the pair with the "hard" process a replacement of (29) should be performed, whereas other pairs of quarks will still interact elastically. It means that, for any integral in the expansion of (B.1) of the elastic amplitude, we will make the following replacement for any term of $P_{q-q}(b_i)\dots P_{q-q}(b_j)$ type:

$$P_{q-q}(b_i)\dots P_{q-q}(b_j) \to \frac{\mathrm{e}^{-\frac{b_i^2}{2R^2_{Q\mathrm{H}}}}}{2\pi R^2_{\mathrm{H}}}\hat{P}_{q-q}(b_i)\dots P_{q-q}(b_j) \quad (33)$$

for each $P_{q-q}(b_k)$ in the chain $P_{q-q}(b_i)\dots P_{q-q}(b_j)$. This procedure is illustrated by Fig. 12 for the case of the interaction of two pairs of quarks.

Performing these replacements and summing all terms, we obtain a new amplitude $\hat{A}(s,b)$ (see (B.1)). In Appendix C we show an example of this procedure for the $A_{3\mathrm{pairs}}(s,b)$ term of the elastic amplitude $A(s,b)$. With this amplitude, $\hat{A}(s,b)$, we determine the "hard" cross section as follows:

$$\sigma_{\mathrm{hard}} \propto \int \mathrm{d}^2b\,(\hat{A}(s,b))^2, \quad (34)$$

where the first term of this expansion has the form

$$\sigma^1_{\mathrm{hard}} \propto \frac{81}{4\pi^2 R^4_{\mathrm{H}}}\int \mathrm{d}^2b\left(\frac{9\alpha^2}{4\pi^2}\int \mathrm{d}^2b_1\int \mathrm{d}^2b_2\,\mathrm{e}^{-\frac{3\alpha}{2}(\mathbf{b}-\mathbf{b}_1)^2}\times\hat{P}_{q-q}(Y,b_2)\mathrm{e}^{-\frac{b_2^2}{2R^2_{Q\mathrm{H}}}}\mathrm{e}^{-\frac{3\alpha}{2}(\mathbf{b}_1-\mathbf{b}_2)^2}\right)^2. \quad (35)$$

Finally, the answer for the survival probability factor in all orders of the expansion of (B.1) looks as follows:

$$\hat{S}^2 = 4\pi^2 R^4_{\mathrm{H}}\int \mathrm{d}^2b\,(\hat{A}(s,b))^2 \Big/ \int \mathrm{d}^2b\left(9\frac{9\alpha^2}{4\pi^2}\int \mathrm{d}^2b_1\int \mathrm{d}^2b_2\times\mathrm{e}^{-\frac{3\alpha}{2}(\mathbf{b}-\mathbf{b}_1)^2}\mathrm{e}^{-\frac{b_2^2}{2R^2_{Q\mathrm{H}}}}\mathrm{e}^{-\frac{3\alpha}{2}(\mathbf{b}_1-\mathbf{b}_2)^2}\right)^2. \quad (36)$$

For example, there is the first term, which contributes to $\hat{S}^2$:

$$\hat{S}^2_1 = \frac{\left(\int \mathrm{d}^2b\left(\frac{9\alpha^2}{4\pi^2}\int \mathrm{d}^2b_1\int \mathrm{d}^2b_2\,\mathrm{e}^{-\frac{3\alpha}{2}(\mathbf{b}-\mathbf{b}_1)^2}\mathrm{e}^{-\frac{b_2^2}{2R^2_{Q\mathrm{H}}}}\times\hat{P}_{q-q}(Y,b_2)\mathrm{e}^{-\frac{3\alpha}{2}(\mathbf{b}_1-\mathbf{b}_2)^2}\right)^2\right)}{\left(\int \mathrm{d}^2b\left(\frac{9\alpha^2}{4\pi^2}\int \mathrm{d}^2b_1\int \mathrm{d}^2b_2\,\mathrm{e}^{-\frac{3\alpha}{2}(\mathbf{b}-\mathbf{b}_1)^2}\times\mathrm{e}^{-\frac{b_2^2}{2R^2_{Q\mathrm{H}}}}\mathrm{e}^{-\frac{3\alpha}{2}(\mathbf{b}_1-\mathbf{b}_2)^2}\right)^2\right)}. \quad (37)$$

The values of the survival probability factor, $\hat{S}^2$, calculated in this approach, are shown in Table 1. We see that these values are close to the values of the survival probability for the central diffraction process calculated in [40]. We also performed the calculation of the integrant in the numerator of (36), which is proportional to the amplitude of the "hard" central diffraction process. The plots of this integrant as a function of the impact parameter at different energies are presented in Fig. 13. Considering these graphs, we conclude that the main contribution to the amplitude of the central diffraction "hard" production comes from the non-central values of the impact parameter, and it is almost zero for the central impact parameter at high energies.

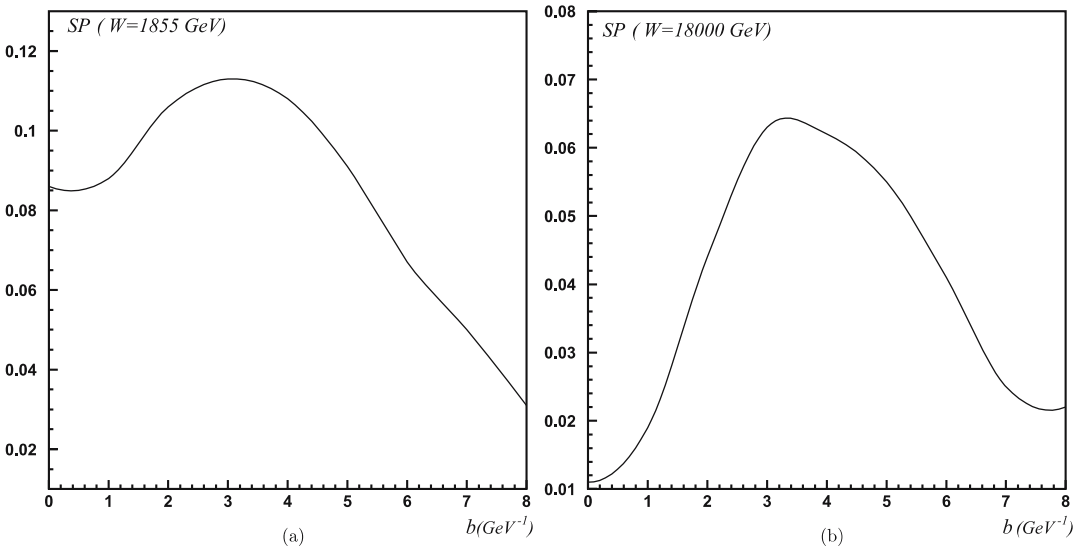

Fig. 13. The impact parameter behavior of the integrant in the numerator of (36) at energies $W = 1855$ GeV and $W = 18\,000$ GeV

6 The cross section of the diffraction dissociation

The elastic amplitude of the considered model accounts for many pomeron exchanges between different pairs of quarks. Now we want to calculate the cross section of the diffraction dissociation processes taking into account all these interactions. The diffractive dissociation (DD) processes for us are all processes in which no particle has been produced in the rapidity region between two scattered protons. From the unitarity constraint we have

$$\sigma_{\rm tot} = \sigma_{\rm el} + \sigma_{\rm inel} + \sigma_{\rm DD}\,. \tag{38}$$

Therefore

$$\sigma_{\rm DD} = \sigma_{\rm tot} - \sigma_{\rm el} - \sigma_{\rm inel}\,. \tag{39}$$

From our previous calculations we know the values of $\sigma_{\rm el}$ and $\sigma_{\rm tot}$. So, in order to calculate $\sigma_{\rm DD}$ we need to calculate the value of $\sigma_{\rm inel}$, and it is clear that, since we do not consider the triple pomeron vertex in our model, $\sigma_{\rm DD}$ contains only the contribution from diffractive processes of the low mass states, whereas the large mass production states are not accounted for in the framework of the calculation.

The calculation of $\sigma_{\rm inel}$ is pretty simple. In first order, where

$$\sigma^1_{\rm tot} = 2\int {\rm d}^2b\,{\rm Im}\,A_{\rm 1pair}(s,b) = 18\int {\rm d}^2b\,P_{q-q}(Y,b)\,, \tag{40}$$

for $\sigma_{\rm inel}$ we have

$$\sigma_{\rm inel} = \int {\rm d}^2b\,A^{\rm inel}_{\rm 1pair}(s,b) = 9\int {\rm d}^2b\,P^{\rm inel}_{q-q}(Y,b)\,, \tag{41}$$

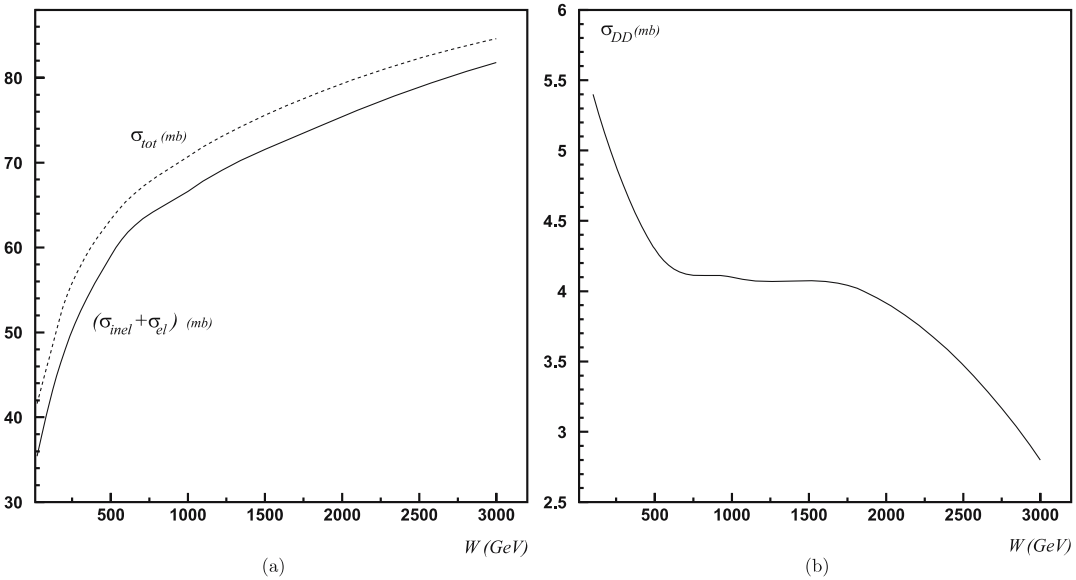

Fig. 14. The sum of elastic and inelastic cross sections in comparison with the total cross section and small mass DD cross section as the function of $W = \sqrt{s}$

Table 2. The low mass diffractive dissociation cross section at high energies as a function of $\sqrt{s}$

$\sigma_{\rm DD}(\sqrt{s}=7000\,{\rm GeV})$	$\sigma_{\rm DD}(\sqrt{s}=10\,000\,{\rm GeV})$	$\sigma_{\rm DD}(\sqrt{s}=15\,000\,{\rm GeV})$	$\sigma_{\rm DD}(\sqrt{s}=18\,000\,{\rm GeV})$
2.3 mb	0.4 mb	0.35 mb	0.3 mb

with

$$P^{\rm inel}_{q-q}(Y,b)=1-{\rm e}^{-\Omega_{q-q}(Y,b)}\,. \tag{42}$$

We perform the calculation of $\sigma_{\rm inel}$ for all possible interactions between the pairs of the quarks in the protons using the following simple recipe. In each expression for $\sigma_{\rm tot}$ for the interactions of the different numbers of quark pairs considered,

$$\sigma_{\rm tot}=2\int {\rm d}^2b\,{\rm Im}\,A(s,b)\,, \tag{43}$$

we make the following replacement:

$$P_{q-q}(Y,b_i)\dots P_{q-q}(Y,b_j)\to\frac{1}{2}P^{\rm inel}_{q-q}(Y,b_i)\dots P^{\rm inel}_{q-q}(Y,b_j)\,, \tag{44}$$

with $P^{\rm inel}_{q-q}$ given by (42). After the calculation of $\sigma_{\rm inel}$ with the help of (41) we obtain the value of $\sigma_{\rm DD}$. The result of the calculations for the energy range $W=100$–$3000\,{\rm GeV}$ is shown in Fig. 14, as well as the sum of the elastic and inelastic cross sections, in comparison with the total cross section.

For energies higher than $W=3000\,{\rm GeV}$, the cross section of the diffractive dissociation process is small (see Table 2). The smallness of the value of the $\sigma_{\rm DD}$ at high energy is a sign of the "blackness" of the process at central impact parameter, when the diffractive dissociation process is to be mostly peripheral. Nevertheless, it is important to notice again that in calculations of DD processes, we neglected the diffraction dissociation processes with large mass production. As was mentioned before, such processes may be described if we introduce in the model the triple pomeron vertex [11]. We did not consider this vertex in our calculations; therefore, our result for the cross section of the DD processes, which is the sum of single diffraction and double diffraction processes, is smaller than it could be in the case that the triple pomeron vertex is included.

7 Conclusion

In this paper we consider the proton–proton interactions in the framework of the constituent quark model at high energies. The typical "soft" process of p–p scattering we described taking into account all interactions between pairs of quarks in the protons, modeling the quark–quark interaction by an eikonal formula. It turns out that in this model the interactions of one, two or three quarks from one proton with two or three quarks from the second proton surprisingly become essential even at low energies. Indeed, if we look at Fig. 9, we see that even at an energy of $\sqrt{s}=23\,{\rm GeV}$ the contribution from the interaction of two pairs of quarks is approximately one third of the contribution of one pair. Of course, at higher energies the contributions of more interacting quark pairs became more important. For example, at LHC energy the interactions of one and two pairs of quarks equally contribute to the elastic amplitude, and at this energy we need to account the contribution of seven quark pairs. This interaction picture leads to a very natural scenario of unitarization. At high energies the contributions from the interaction of one and two pairs of quarks cancel each other, and the final amplitude at given impact parameter is smaller than one (see Fig. 10). Due to this interaction structure the amplitude has a maximum at $b\approx 2\,{\rm GeV}^{-1}$ at high energy, which means that elastic production is mostly peripheral at high energies. We see also that in this case unitarization is achieved by exploring the internal structure of the proton rather than details of the interactions. Another result, observed in the present model and related to the unitarization of the amplitude, is the relatively small value of the amplitude at zero impact parameter. Indeed, even at an energy of $\sqrt{s}=18\,000\,{\rm GeV}$ at $b=0$ the amplitude is not close to one. The interactions are still "gray" and not "black". Many pomeron interactions between different quark configurations in both protons lead to the "black" picture in the quark–quark interactions but to the "gray" picture in the proton–proton interaction. In spite of the "black" contributions of one, two or three interacting quark pairs, the protons at central impact parameter stay "gray." However, we should stress that in our calculations we assumed that the quark–quark interaction is described by the eikonal approach. This specific mechanism manifests itself in the form of the b dependence of the amplitude, which is quite different from the usual b dependence. We also considered the Gaussian form for the quark impact factors, which also could affect the final form of the elastic amplitude. It is possible that inclusion in the consideration of more realistic quark–pomeron impact factors as well as triple pomeron vertices will change the picture of the proton–proton interactions in CQM.

The model considered in the paper fits the experimental data pretty well (see Fig. 7). Using the parameters of the "input" pomeron, which we obtained through fitting of the data, we can predict the values of the cross sections at high energies. Doing so, we did not find a deviation of the behavior of the elastic slope, $B_{\rm el}$, from the simple linear parameterization (see the plot of Fig. 8). The explanation of this effect is the following. In spite of the hope that the constituent quarks will have strong overlap at high energies and this effect will change the energy behavior of $B_{\rm el}$, it actually does not happen. The value of the size of the constituent quark obtained from the data fit is small,

$R^2_{\rm quark} \approx 0.16\,{\rm GeV}^{-2}$. The slope of the initial quark–quark amplitude, which is our "input" pomeron, also turns out to be small, $\alpha' \approx 0.08\,{\rm GeV}^{-2}$. Therefore, even at an energy of $\sqrt{s} = 18\,000\,{\rm GeV}$ we obtain for the radius of the constituent quark $R_{\rm quark} \approx 0.3$–$0.4\,{\rm fm}$, which is still two times smaller than the radius of the proton. This again supports the conclusion that our interactions at LHC energy are still far from the "black" disk limit.

We also calculated the survival probability factor for different energies, and it turns out to be similar to the values obtained in the model proposed in [40]. The parameters of the "input" pomeron in our paper and in [40] are close, in spite of the fact that we did not involve any non-perturbative physics in our calculations. The intercept of the "input" pomeron that we obtained is $\Delta \approx 0.12$. This intercept is larger than the intercept of [40]. The slope, $\alpha' \approx 0.08\,{\rm GeV}^{-2}$, is very close to the one of [40]. Considering the impact parameter dependence of the amplitude of the exclusive central diffraction "hard" process, see Fig. 13, we see that the maximum of the amplitude is located at the peripheral impact parameter $b \approx 3\,{\rm GeV}^{-2}$ at the energy of LHC. The probability of this process at very central impact parameter is almost zero. The calculations of the cross section of small mass diffractive dissociation, see Fig. 14 and Table 2, support this conclusion. This cross section is very small at high energy, which reflects the "blackness" of the interactions at central impact parameter at high energy, when diffractive processes became mostly peripheral.

The values of the parameters of our "input" pomeron, the slope ($\alpha'_P \approx 0.08\,{\rm GeV}^{-2}$) and the intercept ($\Delta \approx 0.12$) give rise to the idea that this pomeron is not "soft" (see [32] for the typical parameters of the soft pomeron). The parameters that we obtained were related to the so called "hard" pomeron. Therefore, one of the results of this paper is the idea that, perhaps, we do not need to introduce a "soft" pomeron in order to describe the "soft" data. Considering the internal structure of the colliding hadrons as well as the unitarization corrections for the amplitude we can describe the p–p data using only one "hard" pomeron.

The present model, SQM, has very interesting properties, allowing us to describe a lot of experimental data and interpet the proton–proton interaction in terms of interacting quarks. A lot of new and interesting information may be obtained on the unitarization of the cross sections and pomeron structure in the framework of the CQM. Nevertheless, there are a lot of further investigations and improvements possible and needed. We hope that the present paper will contribute to the understanding of hadron–hadron interactions in terms of constituent quarks and that further work in this direction will be continued.

Acknowledgements. We want to thank Asher Gotsman, Uri Maor and Alex Prygarin for very useful discussions on the subject of this paper. This research was supported in part by the Israel Science Foundation, founded by the Israeli Academy of Science and Humanities and by BSF grant #20004019, and the research of S.B. was supported by the Minerva Israel–Germany Science foundation.

Appendix A

In this appendix, we calculate as an example of our calculations two diagrams that contribute to the elastic amplitude: the first diagram of Fig. 15 and the first diagram of Fig. 16.

We begin with the first diagram of Fig. 15. There are six diagrams of this type, and we need two vertices (see (6) and (8)) for the calculations:

$$V_{\rm up}(k) = {\rm e}^{-k^2/(6\alpha)},$$

and

$$V_{\rm down}(k) = {\rm e}^{-\frac{1}{8\alpha}(\mathbf{q}_2-\mathbf{q}_3)^2-\frac{1}{6\alpha}(\mathbf{q}_1-\mathbf{q}_2/2-\mathbf{q}_3/2)^2},$$

where q_i is the momentum transferred of each single pomeron, and $k = q_1 + q_2 + q_3$. So, we have for our diagram

$$D_{1,3{\rm pairs}}(k) = 6\int\prod_{i=1}^{3}\frac{{\rm d}^2q_i}{4\pi^2}P_{q\text{–}q}(q_i){\rm e}^{-k^2/(6\alpha)} \times {\rm e}^{-\frac{1}{8\alpha}(\mathbf{q}_2-\mathbf{q}_3)^2-\frac{3}{8\alpha}(\mathbf{q}_1-\mathbf{k}/3)^2} \times \left(4\pi^2\delta^2(\mathbf{k}-\mathbf{q}_1-\mathbf{q}_2-\mathbf{q}_3)\right), \tag{A.1}$$

where $P_{q\text{–}q}(q_i)$ is the Fourier transform of the amplitude given by (3).

Since we have no simple analytic expression for $P_{q\text{–}q}(q_i)$, we make a Fourier transformation for each function $P_{q\text{–}q}(q_i)$ and rewrite our expression in terms of $P_{q\text{–}q}(b_i)$:

$$P_{q\text{–}q}(q_i) = \int {\rm d}^2b_i\, P_{q\text{–}q}(b_i){\rm e}^{{\rm i}\mathbf{q}_i\mathbf{b}_i}. \tag{A.2}$$

Here b_i is the impact parameter variable, which is conjugate to the momentum q_i of the single pomeron. We also

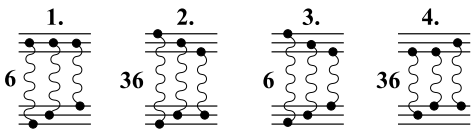

Fig. 15. Four diagrams of the three quark pair interaction. The *wave line* describes the eikonal amplitude for quark–quark interaction $P(Y, b)$

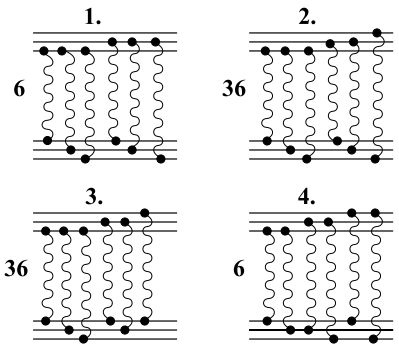

Fig. 16. Four diagrams of the six quark pairs interactions

make a Fourier transformation from k to the impact parameter variable b. We obtain

$$D_{1,3\text{pairs}}(b) = \frac{6}{64\pi^6}\int\prod_{i=1}^{3}\mathrm{d}^2b_i\,P_{q-q}(b_i)\int\prod_{i=1}^{3}\mathrm{d}^2q_i \times\int\mathrm{d}^2k\,\mathrm{e}^{-\mathrm{i}\mathbf{kb}}\mathrm{e}^{\mathrm{i}\sum_{i=1}^{3}\mathbf{q}_i\mathbf{b}_i}\mathrm{e}^{-k^2/(6\alpha)} \times\mathrm{e}^{-\frac{1}{8\alpha}(\mathbf{q}_2-\mathbf{q}_3)^2-\frac{3}{8\alpha}(\mathbf{q}_1-\mathbf{k}/3)^2} \times\delta^2(\mathbf{k}-\mathbf{q}_1-\mathbf{q}_2-\mathbf{q}_3)\,. \tag{A.3}$$

To make this expression easier for our calculations we introduce the new variables

$$x_1 = q_2-q_3\,;\quad x_2 = q_1-k/3\,;\quad x_3 = q_3\,,\\ q_1 = x_2+k/3\,;\quad q_2 = x_1+x_3\,;\quad q_3 = x_3\,. \tag{A.4}$$

The Jacobian of this transformations is equal to unity; we obtain

$$D_{1,3\text{pairs}}(b) = \frac{6}{64\pi^6}\int\prod_{i=1}^{3}\mathrm{d}^2b_i\,P_{q-q}(b_i)\int\prod_{i=1}^{3}\mathrm{d}^2x_i \times\int\mathrm{d}^2k\,\mathrm{e}^{-\mathrm{i}\mathbf{kb}}\mathrm{e}^{\mathrm{i}\mathbf{b}_1(\mathbf{x}_2+\mathbf{k}/3)}\mathrm{e}^{\mathrm{i}\mathbf{b}_2(\mathbf{x}_3+\mathbf{x}_1)}\mathrm{e}^{\mathrm{i}\mathbf{b}_3\mathbf{x}_3} \times\mathrm{e}^{-\frac{1}{6\alpha}k^2-\frac{1}{8\alpha}x_1^2-\frac{3}{8\alpha}x_2^2} \times\delta^2(2\mathbf{k}/3-\mathbf{x}_1-\mathbf{x}_2-2\mathbf{x}_3)\,. \tag{A.5}$$

Performing the x_3 integration we have

$$D_{1,3\text{pairs}}(b) = \frac{6}{4\cdot64\pi^6}\int\prod_{i=1}^{3}\mathrm{d}^2b_i\,P_{q-q}(b_i)\int\prod_{i=1}^{2}\mathrm{d}^2x_i \times\int\mathrm{d}^2k\,\mathrm{e}^{\mathrm{i}\mathbf{k}(-\mathbf{b}+\mathbf{b}_1/3+\mathbf{b}_2/3+\mathbf{b}_3/3)} \times\mathrm{e}^{\mathrm{i}\mathbf{x}_1(\mathbf{b}_2/2-\mathbf{b}_3/2)}\mathrm{e}^{\mathrm{i}\mathbf{x}_2(\mathbf{b}_1-\mathbf{b}_2/2-\mathbf{b}_3/2)} \times\mathrm{e}^{-\frac{1}{6\alpha}k^2-\frac{1}{8\alpha}x_1^2-\frac{3}{8\alpha}x_2^2}. \tag{A.6}$$

Performing one integration over x_i and k, we obtain the final answer for this diagram:

$$D_{1,3\text{pairs}}(b) = \frac{6\alpha^3}{2\pi^3}\int\prod_{i=1}^{3}\mathrm{d}^2b_i\,P_{q-q}(b_i) \times\mathrm{e}^{-\frac{3\alpha}{2}(\mathbf{b}-\mathbf{b}_1/3-\mathbf{b}_2/3-\mathbf{b}_3/3)^2-\frac{\alpha}{2}(\mathbf{b}_2-\mathbf{b}_3)^2-\frac{2\alpha}{3}(\mathbf{b}_1-\mathbf{b}_2/2-\mathbf{b}_3/2)^2}. \tag{A.7}$$

As a second example of the calculational technique we calculate the first diagram of Fig. 16. The main steps in the calculation of this diagram are the same as in the calculation of the first diagram of Fig. 15. Therefore, now we are not focused on the detailed explanation of the main steps, but we rather clarify the principal points of the calculations technique.

Two vertices of the pomerons–quarks coupling have the following form (see (7) and (8)):

$$V_{\text{up}}(k) = \mathrm{e}^{-\frac{1}{6\alpha}(\mathbf{q}_1+\mathbf{q}_2+\mathbf{q}_3)^2-\frac{1}{6\alpha}(\mathbf{q}_4+\mathbf{q}_5+\mathbf{q}_6)^2+\frac{1}{6\alpha}(\mathbf{q}_1+\mathbf{q}_2+\mathbf{q}_3)(\mathbf{q}_4+\mathbf{q}_5+\mathbf{q}_6)},$$

and

$$V_{\text{down}}(k) = \mathrm{e}^{-\frac{1}{8\alpha}(\mathbf{q}_1+\mathbf{q}_4-\mathbf{q}_2-\mathbf{q}_5)^2-\frac{1}{6\alpha}(\mathbf{q}_3+\mathbf{q}_6-\mathbf{q}_1/2-\mathbf{q}_2/2-\mathbf{q}_4/2-\mathbf{q}_5/2)^2}.$$

Here, the total momentum transferred is $k=\sum_{i=1}^{6}q_i$. We change variables, in order to obtain a simple Gaussian expression for these vertices:

$$x_1-x_2 = q_1+q_2+q_3\,,\quad x_1+x_2 = q_4+q_5+q_6\,;\\ x_3 = q_1+q_4-q_2-q_5\,,\quad x_4 = 3q_3/2+3q_6/2-k/2\,;\\ x_5 = q_5\,,\quad x_6 = q_6\,. \tag{A.8}$$

For the old variables q_i and k we have

$$k = 2x_1\,,\\ q_1 = -x_1/3-x_2+x_3/2-x_4/3+x_5+x_6\,;\\ q_2 = 2x_1/3-x_3/2-x-4/3-x_5\,,\\ q_3 = 2x_4/3-x_6+2x_1/3\,;\\ q_4 = x_1+x_2-x_5-x_6\,,\quad q_5 = x_5\,,\quad q_6 = x_6\,. \tag{A.9}$$

Here the momenta q_1 are not independent. For these momenta we used the delta function constraint

$$q_1 = k-q_2-q_3-q_4-q_5-q_6\,.$$

Using (A.9) we calculate the Jacobian of the variable change; it is equal to $\frac{4}{9}$. In the new variables the vertices look very simple:

$$V_{\text{up}}(k) = \mathrm{e}^{-\frac{1}{6\alpha}x_1^2-\frac{1}{2\alpha}x_2^2}, \tag{A.10}$$

$$V_{\text{down}}(k) = \mathrm{e}^{-\frac{1}{8\alpha}x_3^2-\frac{1}{6\alpha}x_4^2}. \tag{A.11}$$

We consider the exponents that stem from the Fourier transformation from momentum to impact parameter representation:

$$\mathrm{e}^{-\mathrm{i}\mathbf{kb}}\mathrm{e}^{\mathrm{i}\prod_{i=1}^{6}\mathbf{q}_i\mathbf{b}_i}, \tag{A.12}$$

where we also have

$$\prod_{i=1}^{6}P_{q-q}(q_i)\to\prod_{i=1}^{6}P_{q-q}(b_i)\,. \tag{A.13}$$

Putting in (A.12) the substitutions of (A.9), we obtain for the exponents of (A.12)

$$\mathrm{e}^{\mathrm{i}\mathbf{x}_1(-2\mathbf{b}+2\mathbf{b}_2/3+2\mathbf{b}_3/3+\mathbf{b}_4-\mathbf{b}_1/3)}\mathrm{e}^{\mathrm{i}\mathbf{x}_2(\mathbf{b}_4-\mathbf{b}_1)} \times\mathrm{e}^{\mathrm{i}\mathbf{x}_3(\mathbf{b}_1/2-\mathbf{b}_2/2)}\mathrm{e}^{\mathrm{i}\mathbf{x}_4(-\mathbf{b}_2/3+2\mathbf{b}_3/3-\mathbf{b}_1/3)} \times\mathrm{e}^{\mathrm{i}\mathbf{x}_5(-\mathbf{b}_2-\mathbf{b}_4+\mathbf{b}_5+\mathbf{b}_1)}\mathrm{e}^{\mathrm{i}\mathbf{x}_6(-\mathbf{b}_3-\mathbf{b}_4+\mathbf{b}_6+\mathbf{b}_1)}. \tag{A.14}$$

The vertices of (A.10) and (A.11) have no dependence on the variables x_5 and x_6. Therefore, in the integration over x_5 and x_6 we obtain the following delta functions:

$$\delta^2(b_5+b_1-b_2-b_4)\to b_5 = b_2+b_4-b_1\,, \tag{A.15}$$

$$\delta^2(b_6+b_1-b_3-b_4)\to b_6 = b_3+b_4-b_1\,. \tag{A.16}$$

In this case, after the integration over b_5 and b_6, the answer for the functions $P_{q\text{–}q}(b_i)$ (see (A.13)) looks as follows:

$$\prod_{i=1}^{6} P_{q\text{–}q}(q_i) \to \prod_{i=1}^{4} P_{q\text{–}q}(b_i) P_{q\text{–}q}(b_2+b_4-b_1) \times P_{q\text{–}q}(b_3+b_4-b_1)\,, \qquad \text{(A.17)}$$

Of course, if we need, we should also replace b_5 and b_6 in the other exponents of (A.14) substituting (A.15) and (A.16). In our particular diagram this replacement is not in order since the exponents of (A.14) do not depend on b_5 and b_6.

We are ready to write the answer for our diagram. Performing a simple integration over the variables x_i, where $i=1,\ldots,4$, we obtain (we use the Gaussian functions of (A.10) and (A.11) with the four exponents of (A.14))

$$\begin{aligned} &D_{1,6\mathrm{Pom}}(b) \\ &= \frac{6\alpha^4}{\pi^4}\int\prod_{i=1}^{4}\mathrm{d}^2b_i P_{q\text{–}q}(b_i)P_{q\text{–}q}(b_2+b_4-b_1) \\ &\times P_{q\text{–}q}(b_3+b_4-b_1) \\ &\times\exp\left[-\frac{3\alpha}{2}(2\mathbf{b}-2\mathbf{b}_2/3-2\mathbf{b}_3/3-\mathbf{b}_4+\mathbf{b}_1/3)^2\right. \\ &\quad -\frac{\alpha}{2}(\mathbf{b}_4-\mathbf{b}_1)^2-\frac{\alpha}{2}(\mathbf{b}_1-\mathbf{b}_2)^2 \\ &\quad \left.-\frac{2\alpha}{3}(\mathbf{b}_3-\mathbf{b}_2/2-\mathbf{b}_1/2)^2\right]. \end{aligned} \qquad \text{(A.18)}$$

We calculate all other diagrams that contribute to the elastic amplitude using the same methods as have been described above. The answer for the entire amplitude, with the expression for all possible diagrams of our model included, is written in Appendix .

Appendix B

In this appendix we present the resulting expressions for the full elastic amplitude, order by order. We have for the amplitude (see (9))

$$\mathrm{Im}\,A(s,b) = \mathrm{Im}\,A_{1\mathrm{pair}}(s,b) - \mathrm{Im}\,A_{2\mathrm{pairs}}(s,b) + \mathrm{Im}\,A_{3\mathrm{pairs}}(s,b) + \ldots + \mathrm{Im}\,A_{9\mathrm{pairs}}(s,b)\,. \qquad \text{(B.1)}$$

The answer for the contribution to the amplitude from one pair of quarks, $A_{1\mathrm{pair}}(s,b)$, is given in (11). So we start from the contribution of two pairs. The diagrams of this contribution are shown in Fig. 17.

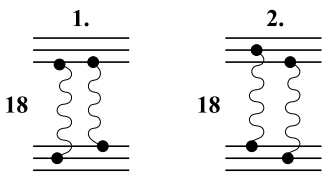

Fig. 17. Two diagrams for the interactions of two quark pairs

We have for $A(s,b)_{2\mathrm{pairs}}$

$$\begin{aligned} \mathrm{Im}\,A_{2\mathrm{pairs}}(s,b) &= \frac{54\alpha^2}{5\pi^2}\int\prod_{i=1}^{2}\mathrm{d}^2b_i\,P_{q\text{–}q}(b_i) \\ &\times \mathrm{e}^{-\frac{6\alpha}{5}(\mathbf{b}_1/2+\mathbf{b}_2/2-\mathbf{b})^2-\frac{\alpha}{2}(\mathbf{b}_1-\mathbf{b}_2)^2} \\ &+\frac{27\alpha^2}{2\pi^2}\int\prod_{i=1}^{2}\mathrm{d}^2b_i\,P_{q\text{–}q}(b_i) \\ &\times \mathrm{e}^{-3\alpha(\mathbf{b}_1/2+\mathbf{b}_2/2-\mathbf{b})^2-\frac{\alpha}{4}(\mathbf{b}_1-\mathbf{b}_2)^2}. \end{aligned} \qquad \text{(B.2)}$$

The diagrams for the three pairs of interacting quarks are shown in Fig. 15. We have for this contribution

$$\begin{aligned} &\mathrm{Im}\,A_{3\mathrm{pairs}}(s,b) \\ &= \frac{6\alpha^3}{2\pi^3}\int\prod_{i=1}^{3}\mathrm{d}^2b_i\,P_{q\text{–}q}(b_i) \\ &\times \mathrm{e}^{-\frac{3\alpha}{2}(\mathbf{b}-\mathbf{b}_1/3-\mathbf{b}_2/3-\mathbf{b}_3/3)^2-\frac{\alpha}{2}(\mathbf{b}_2-\mathbf{b}_3)^2-\frac{2\alpha}{3}(\mathbf{b}_1-\mathbf{b}_2/2-\mathbf{b}_3/2)^2} \\ &+\frac{27\alpha^3}{\pi^3}\int\prod_{i=1}^{3}\mathrm{d}^2b_i\,P_{q\text{–}q}(b_i) \\ &\times \mathrm{e}^{-\frac{\alpha}{2}(3\mathbf{b}-\mathbf{b}_1-\mathbf{b}_2-\mathbf{b}_3)^2-\frac{\alpha}{2}(\mathbf{b}_2-\mathbf{b}_1)^2-\frac{3\alpha}{4}(\mathbf{b}-\mathbf{b}_3)^2} \\ &+\frac{9\alpha^3}{\pi^3}\int\prod_{i=1}^{2}\mathrm{d}^2b_i\,P_{q\text{–}q}(b_i)P_{q\text{–}q}(3b-b_2-b_1) \\ &\times \mathrm{e}^{-\frac{\alpha}{3}(3\mathbf{b}-3\mathbf{b}_1/2-3\mathbf{b}_2/2)^2-\frac{\alpha}{4}(\mathbf{b}_2-\mathbf{b}_1)^2} \\ &+\frac{27\alpha^3}{\pi^3}\int\prod_{i=1}^{3}\mathrm{d}^2b_i\,P_{q\text{–}q}(b_i) \\ &\times \mathrm{e}^{-3\alpha(\mathbf{b}-\mathbf{b}_2/2-\mathbf{b}_3/2)^2-\frac{\alpha}{2}(\mathbf{b}_2-\mathbf{b}_1)^2-\frac{\alpha}{2}(\mathbf{b}_1-\mathbf{b}_3)^2}. \end{aligned} \qquad \text{(B.3)}$$

For the amplitude corresponding to four pairs we have the diagrams of Fig. 18.

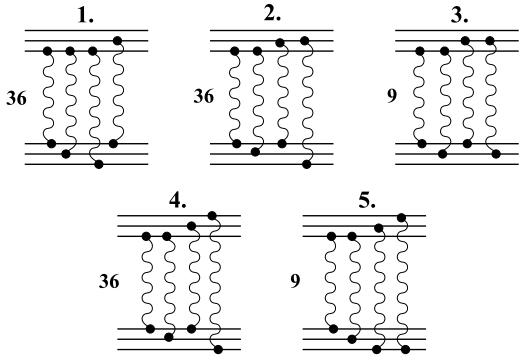

Fig. 18. Five diagrams for interactions of four quark pairs

For this contribution we have

$$
\begin{aligned}
&\mathrm{Im}\, A_{4\mathrm{pairs}}(s,b)\\
&= \frac{36\alpha^4}{\pi^4}\int\prod_{i=1}^{4}\mathrm{d}^2b_i P_{q-q}(b_i)\\
&\quad\times\exp\Big[-\frac{\alpha}{6}(6\mathbf{b}+\mathbf{b}_1-2\mathbf{b}_2-2\mathbf{b}_3-3\mathbf{b}_4)^2\\
&\qquad-\frac{\alpha}{2}(\mathbf{b}_1-\mathbf{b}_4)^2\\
&\qquad-\frac{\alpha}{2}(\mathbf{b}_1-\mathbf{b}_2)^2-\frac{3\alpha}{2}(\mathbf{b}_1/3+\mathbf{b}_2/3-2\mathbf{b}_3/3)^2\Big]\\
&\quad+\frac{36\alpha^4}{\pi^4}\int\prod_{i=1}^{4}\mathrm{d}^2b_i P_{q-q}(b_i)\\
&\quad\times\exp\Big[-\frac{\alpha}{6}(6\mathbf{b}-\mathbf{b}_1-2\mathbf{b}_2-\mathbf{b}_3-2\mathbf{b}_4)^2\\
&\qquad-\frac{\alpha}{2}(\mathbf{b}_1-\mathbf{b}_3)^2\\
&\qquad-\frac{\alpha}{2}(\mathbf{b}_1-\mathbf{b}_2)^2-\frac{2\alpha}{3}(\mathbf{b}_1/2-\mathbf{b}_2/2-\mathbf{b}_3+\mathbf{b}_4)^2\Big]\\
&\quad+\frac{27\alpha^4}{4\pi^4}\int\prod_{i=1}^{3}\mathrm{d}^2b_i P_{q-q}(b_i)P_{q-q}(b_1-b_2-b_3)\\
&\quad\times\mathrm{e}^{-\frac{3\alpha}{4}(2\mathbf{b}-\mathbf{b}_2-\mathbf{b}_3)^2-\frac{\alpha}{2}(\mathbf{b}_1-\mathbf{b}_3)^2-\frac{\alpha}{2}(\mathbf{b}_1-\mathbf{b}_2)^2}\\
&\quad+\frac{27\alpha^4}{4\pi^4}\int\prod_{i=1}^{3}\mathrm{d}^2b_i P_{q-q}(b_i)P_{q-q}(3b-b_2-b_3)\\
&\quad\times\mathrm{e}^{-\frac{3\alpha}{4}(2\mathbf{b}-\mathbf{b}_2-\mathbf{b}_3)^2-\frac{\alpha}{2}(\mathbf{b}_1-\mathbf{b}_3)^2-\frac{\alpha}{2}(\mathbf{b}_1-\mathbf{b}_2)^2}\\
&\quad+\frac{9\alpha^4}{\pi^4}\int\prod_{i=1}^{4}\mathrm{d}^2b_i P_{q-q}(b_i)\\
&\quad\times\exp\Big[-\frac{3\alpha}{4}(4\mathbf{b}-\mathbf{b}_1-\mathbf{b}_2-\mathbf{b}_3-\mathbf{b}_4)^2\\
&\qquad-\frac{\alpha}{2}(\mathbf{b}_4-\mathbf{b}_3)^2-\frac{\alpha}{2}(\mathbf{b}_1-\mathbf{b}_2)^2\\
&\qquad-\frac{\alpha}{12}(\mathbf{b}_1+\mathbf{b}_2-\mathbf{b}_3-\mathbf{b}_4)^2\Big]\,. \qquad \text{(B.4)}
\end{aligned}
$$

The five pair interaction diagrams are shown in Fig. 19.

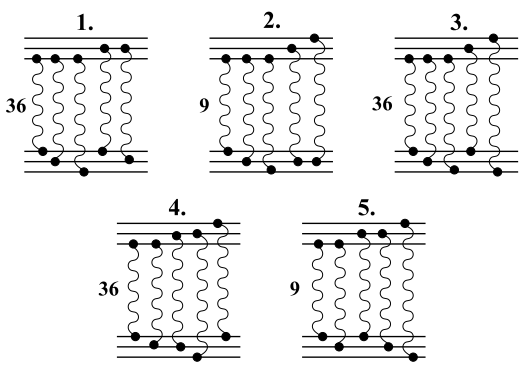

Fig. 19. Five diagrams for the interactions of five quark pairs

In this case we have

$$
\begin{aligned}
&\mathrm{Im}\, A_{5\mathrm{pairs}}(s,b)\\
&= \frac{36\alpha^4}{\pi^4}\int\prod_{i=1}^{4}\mathrm{d}^2b_i\, P_{q-q}(b_i)P_{q-q}(b_2+b_4-b_1)\\
&\quad\times\exp\Big[-\frac{3\alpha}{2}(2\mathbf{b}+\mathbf{b}_1/3-2\mathbf{b}_2/3-2\mathbf{b}_3/3-\mathbf{b}_4)^2\\
&\qquad-\frac{\alpha}{2}(\mathbf{b}_1-\mathbf{b}_4)^2-\frac{\alpha}{2}(\mathbf{b}_1-\mathbf{b}_2)^2\\
&\qquad-\frac{2\alpha}{3}(\mathbf{b}_1+\mathbf{b}_2-\mathbf{b}_3)^2\Big]\\
&\quad+\frac{9\alpha^4}{\pi^4}\int\prod_{i=1}^{4}\mathrm{d}^2b_i\, P_{q-q}(b_i)P_{q-q}(3b-b_1+b_2-b_3-b_4)\\
&\quad\times\exp\Big[-\frac{2\alpha}{3}(3\mathbf{b}/2-\mathbf{b}_1/2+\mathbf{b}_2-3\mathbf{b}_3/2-\mathbf{b}_4/2)^2\\
&\qquad-\frac{\alpha}{2}(\mathbf{b}_2-\mathbf{b}_4)^2-\frac{\alpha}{2}(3\mathbf{b}-\mathbf{b}_1-\mathbf{b}_3-\mathbf{b}_4)^2\\
&\qquad-\frac{2\alpha}{3}(\mathbf{b}_1-\mathbf{b}_2/2-\mathbf{b}_4/2)^2\Big]\\
&\quad+\frac{36\alpha^4}{\pi^4}\int\prod_{i=1}^{4}\mathrm{d}^2b_i\, P_{q-q}(b_i)P_{q-q}(3b-b_2-b_4)\\
&\quad\times\exp\Big[-\frac{2\alpha}{3}(3\mathbf{b}/2-\mathbf{b}_1/2-\mathbf{b}_2-\mathbf{b}_3/2-\mathbf{b}_4)^2\\
&\qquad-\frac{\alpha}{2}(\mathbf{b}_1-\mathbf{b}_4)^2-\frac{\alpha}{2}(\mathbf{b}_1-\mathbf{b}_3)^2\\
&\qquad-\frac{2\alpha}{3}(\mathbf{b}_1/2+\mathbf{b}_2-\mathbf{b}_3-\mathbf{b}_4/2)^2\Big]\\
&\quad+\frac{36\alpha^4}{\pi^4}\int\prod_{i=1}^{4}\mathrm{d}^2b_i\, P_{q-q}(b_i)P_{q-q}(3b-b_2-b_4)\\
&\quad\times\exp\Big[-\frac{2\alpha}{3}(3\mathbf{b}-\mathbf{b}_1-\mathbf{b}_2/2-\mathbf{b}_3/2-\mathbf{b}_4)^2\\
&\qquad-\frac{\alpha}{2}(\mathbf{b}_1-\mathbf{b}_2)^2-\frac{\alpha}{2}(\mathbf{b}_2-\mathbf{b}_3)^2\\
&\qquad-\frac{2\alpha}{3}(\mathbf{b}_1/2-\mathbf{b}_2/2+\mathbf{b}_3-\mathbf{b}_4)^2\Big]\\
&\quad+\frac{27\alpha^3}{16\pi^3}\int\prod_{i=1}^{3}\mathrm{d}^2b_i\, P_{q-q}(b_i)P_{q-q}(3b-b_2-b_3)\\
&\quad\times P_{q-q}(b_1-b_2-b_3)\\
&\quad\times\exp\Big[-\frac{3\alpha}{4}(2\mathbf{b}-\mathbf{b}_2-\mathbf{b}_3)^2-\frac{\alpha}{2}(\mathbf{b}_1-\mathbf{b}_2)^2\\
&\qquad-\frac{\alpha}{4}(\mathbf{b}_2-\mathbf{b}_3)^2-\frac{\alpha}{3}(\mathbf{b}_1-\mathbf{b}_2/2-\mathbf{b}_3/2)^2\Big]\,. \qquad \text{(B.5)}
\end{aligned}
$$

The diagrams with the interaction of six quark pairs are shown in Fig. 16. For this contribution we have

$$
\begin{aligned}
&\mathrm{Im}\, A_{6\mathrm{pairs}}(s,b)\\
&= \frac{6\alpha^4}{\pi^4}\int\prod_{i=1}^{4}\mathrm{d}^2b_i\, P_{q-q}(b_i)P_{q-q}(b_2+b_4-b_1)\\
&\quad\times P_{q-q}(b_3+b_4-b_1)
\end{aligned}
$$

$$
\begin{aligned}
&\times \exp\left[-\frac{3\alpha}{2}(2\mathbf{b}-2\mathbf{b}_2/3-2\mathbf{b}_3/3-\mathbf{b}_4+\mathbf{b}_1/3)^2\right.\\
&\qquad -\frac{\alpha}{2}(\mathbf{b}_4-\mathbf{b}_1)^2-\frac{\alpha}{2}(\mathbf{b}_1-\mathbf{b}_2)^2\\
&\qquad \left.-\frac{2\alpha}{3}(\mathbf{b}_3-\mathbf{b}_2/2-\mathbf{b}_1/2)^2\right]\\
&+\frac{36\alpha^4}{\pi^4}\int\prod_{i=1}^{4}\mathrm{d}^2b_i\,P_{q\text{-}q}(b_i)P_{q\text{-}q}(3b-b_2-b_4)\\
&\times P_{q\text{-}q}(b_2+b_4-b_1)\\
&\times \exp\left[-\frac{2\alpha}{3}(3\mathbf{b}-\mathbf{b}_1/2-\mathbf{b}_2+\mathbf{b}_3-3\mathbf{b}_4/2)^2\right.\\
&\qquad -\frac{\alpha}{2}(\mathbf{b}_2-\mathbf{b}_1)^2-\frac{\alpha}{2}(\mathbf{b}_1-\mathbf{b}_4)^2\\
&\qquad \left.-\frac{2\alpha}{3}(\mathbf{b}_3-\mathbf{b}_1-\mathbf{b}_2)^2\right]\\
&+\frac{36\alpha^4}{\pi^4}\int\prod_{i=1}^{4}\mathrm{d}^2b_i\,P_{q\text{-}q}(b_i)P_{q\text{-}q}(3b+b_1-b_2-b_3-b_4)\\
&\times P_{q\text{-}q}(b_2+b_4-b_1)\\
&\times \exp\left[-\frac{2\alpha}{3}(3\mathbf{b}+\mathbf{b}_1/2-\mathbf{b}_2-\mathbf{b}_3-3\mathbf{b}_4/2)^2\right.\\
&\qquad -\frac{\alpha}{2}(\mathbf{b}_2-\mathbf{b}_1)^2-\frac{\alpha}{2}(\mathbf{b}_1-\mathbf{b}_4)^2\\
&\qquad \left.-\frac{2\alpha}{3}(\mathbf{b}_3-\mathbf{b}_1/2-\mathbf{b}_2/2)^2\right]\\
&+\frac{6\alpha^4}{\pi^4}\int\prod_{i=1}^{4}\mathrm{d}^2b_i\,P_{q\text{-}q}(b_i)P_{q\text{-}q}(3b-b_2-b_4)\\
&\times P_{q\text{-}q}(3b-b_1-b_3)\\
&\times \exp\left[-\frac{2\alpha}{3}(3\mathbf{b}-\mathbf{b}_1-\mathbf{b}_2/2-\mathbf{b}_3/2-\mathbf{b}_4)^2\right.\\
&\qquad -\frac{\alpha}{2}(\mathbf{b}_2-\mathbf{b}_1)^2-\frac{\alpha}{2}(\mathbf{b}_2-\mathbf{b}_3)^2\\
&\qquad \left.-\frac{2\alpha}{3}(\mathbf{b}_4-\mathbf{b}_3-\mathbf{b}_1/2+\mathbf{b}_2/2)^2\right]. \qquad \text{(B.6)}
\end{aligned}
$$

The diagrams with the interaction of seven quark pairs are shown in Fig. 20.

For these diagrams we have

$$
\begin{aligned}
&\mathrm{Im}\,A_{7\mathrm{pairs}}(s,b)\\
&=\frac{18\alpha^4}{\pi^4}\int\prod_{i=1}^{4}\mathrm{d}^2b_i\,P_{q\text{-}q}(b_i)P_{q\text{-}q}(2b-b_4-b_3)\\
&\times P_{q\text{-}q}(b_2+b_4-b_1)P_{q\text{-}q}(b_1-b_2+b_3)\\
&\times \exp\left[-\frac{2\alpha}{3}(3\mathbf{b}-\mathbf{b}_1/2-\mathbf{b}_2/2-\mathbf{b}_3-\mathbf{b}_4)^2\right.\\
&\qquad -\frac{\alpha}{2}(\mathbf{b}_4-\mathbf{b}_1)^2-\frac{\alpha}{2}(\mathbf{b}_1-\mathbf{b}_2)^2\\
&\qquad \left.-\frac{2\alpha}{3}(\mathbf{b}_3-\mathbf{b}_2+\mathbf{b}_1/2-\mathbf{b}_4/2)^2\right]\\
&+\frac{18\alpha^4}{\pi^4}\int\prod_{i=1}^{4}\mathrm{d}^2b_i\,P_{q\text{-}q}(b_i)P_{q\text{-}q}(3b-b_4-b_3)\\
&\times P_{q\text{-}q}(3b-b_4-b_2)P_{q\text{-}q}(b_2-b_1+b_4)\\
&\times \exp\left[-\frac{2\alpha}{3}(3\mathbf{b}+3\mathbf{b}_1/2-\mathbf{b}_2-\mathbf{b}_3-3\mathbf{b}_4/2)^2\right.\\
&\qquad -\frac{\alpha}{2}(\mathbf{b}_4-\mathbf{b}_1)^2-\frac{\alpha}{2}(\mathbf{b}_1-\mathbf{b}_2)^2\\
&\qquad \left.-\frac{2\alpha}{3}(\mathbf{b}_3-\mathbf{b}_2/2-\mathbf{b}_1/2)^2\right]. \qquad \text{(B.7)}
\end{aligned}
$$

Finally, there is only one type of diagram with interactions for eight and nine quark pairs (see Fig. 21).

So we have for the diagrams with the interaction of eight quark pairs

$$
\begin{aligned}
&\mathrm{Im}\,A_{8\mathrm{pairs}}(s,b)\\
&=\frac{\alpha^4}{\pi^4}\int\prod_{i=1}^{4}\mathrm{d}^2b_i\,P_{q\text{-}q}(b_i)P_{q\text{-}q}(2b-b_1)P_{q\text{-}q}(2b-b_2)\\
&\times P_{q\text{-}q}(2b-b_1-b_2-b_3)P_{q\text{-}q}(b_1-b_2+b_4)\\
&\times \exp\left[-\frac{2\alpha}{3}(\mathbf{b}-\mathbf{b}_1/2+\mathbf{b}_2/2-\mathbf{b}_4)^2\right.\\
&\qquad -\frac{\alpha}{2}(\mathbf{b}_2-\mathbf{b}_1)^2-\frac{\alpha}{2}(2\mathbf{b}-\mathbf{b}_1-\mathbf{b}_2)^2\\
&\qquad \left.-\frac{2\alpha}{3}(2\mathbf{b}-\mathbf{b}_1/2-\mathbf{b}_2/2-\mathbf{b}_3)^2\right], \qquad \text{(B.8)}
\end{aligned}
$$

and the diagram for nine quark pair interactions gives

$$
\begin{aligned}
&\mathrm{Im}\,A_{9\mathrm{pairs}}(s,b)\\
&=\frac{\alpha^4}{9\pi^4}\int\prod_{i=1}^{4}\mathrm{d}^2b_i\,P_{q\text{-}q}(b_i)P_{q\text{-}q}(2b-b_1)P_{q\text{-}q}(2b-b_4)\\
&\times P_{q\text{-}q}(2b-b_1+b_2-b_4)P_{q\text{-}q}(b_3-b_2+b_4)
\end{aligned}
$$

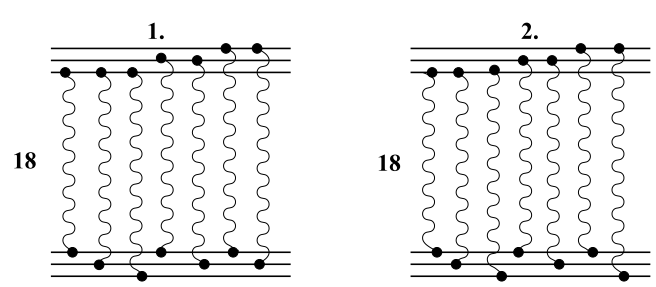

Fig. 20. Two diagrams for the interactions of seven quark pairs

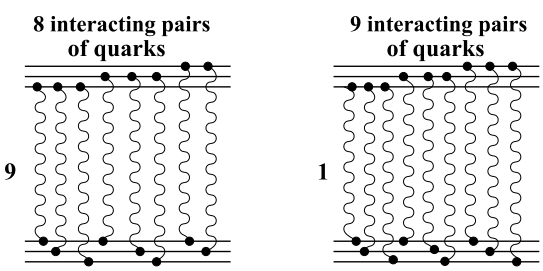

Fig. 21. Two diagrams for the interactions of eight and nine quark pairs

$$\times P_{q-q}(b_1-b_2-b_3)$$
$$\times \exp\left[-\frac{2\alpha}{3}(\mathbf{b}+\mathbf{b}_1/2-\mathbf{b}_3-\mathbf{b}_4/2)^2 - \frac{\alpha}{2}(\mathbf{b}_4-\mathbf{b}_1)^2 - \frac{\alpha}{2}(2\mathbf{b}-\mathbf{b}_1-\mathbf{b}_4)^2 - \frac{2\alpha}{3}(\mathbf{b}_1/2-\mathbf{b}_2-\mathbf{b}_4/2)^2\right]. \quad \text{(B.9)}$$

In our numerical calculations we used only the $\mathrm{Im}\,A(s,b)_{1\mathrm{pair}}$–$\mathrm{Im}\,A(s,b)_{7\mathrm{pairs}}$ terms of the amplitude. The terms $\mathrm{Im}\,A(s,b)_{6\mathrm{pairs}}$ and $\mathrm{Im}\,A(s,b)_{7\mathrm{pairs}}$ are important only at energies close to the LHC one.

Appendix C

As an example of an expression for the calculation of the survival probability in the framework of our approach we consider the term of the elastic amplitude with three interacting quark pairs:

$$\begin{aligned}
&\mathrm{Im}\,A(s,b)_{3\mathrm{pairs}} \\
&= \frac{6\alpha^3}{2\pi^3}\int\prod_{i=1}^{3}\mathrm{d}^2b_i\,P_{q-q}(b_i) \\
&\times \mathrm{e}^{-\frac{3\alpha}{2}(\mathbf{b}-\mathbf{b}_1/3-\mathbf{b}_2/3-\mathbf{b}_3/3)^2-\frac{\alpha}{2}(\mathbf{b}_2-\mathbf{b}_3)^2-\frac{2\alpha}{3}(\mathbf{b}_1-\mathbf{b}_2/2-\mathbf{b}_3/2)^2} \\
&+ \frac{27\alpha^3}{\pi^3}\int\prod_{i=1}^{3}\mathrm{d}^2b_i\,P_{q-q}(b_i) \\
&\times \mathrm{e}^{-\frac{\alpha}{2}(3\mathbf{b}-\mathbf{b}_1-\mathbf{b}_2-\mathbf{b}_3)^2-\frac{\alpha}{2}(\mathbf{b}_2-\mathbf{b}_1)^2-\frac{3\alpha}{4}(\mathbf{b}-\mathbf{b}_3)^2} \\
&+ \frac{9\alpha^3}{\pi^3}\int\prod_{i=1}^{2}\mathrm{d}^2b_i\,P_{q-q}(b_i)P_{q-q}(3b-b_2-b_1) \\
&\times \mathrm{e}^{-\frac{\alpha}{3}(3\mathbf{b}-3\mathbf{b}_1/2-3\mathbf{b}_2/2)^2-\frac{\alpha}{4}(\mathbf{b}_2-\mathbf{b}_1)^2} \\
&+ \frac{27\alpha^3}{\pi^3}\int\prod_{i=1}^{3}\mathrm{d}^2b_i\,P_{q-q}(b_i) \\
&\times \mathrm{e}^{-3\alpha(\mathbf{b}-\mathbf{b}_2/2-\mathbf{b}_3/2)^2-\frac{\alpha}{2}(\mathbf{b}_2-\mathbf{b}_1)^2-\frac{\alpha}{2}(\mathbf{b}_1-\mathbf{b}_3)^2}. \qquad \text{(C.1)}
\end{aligned}$$

Let us rewrite the first term of this expression. Using the recipe of (33), we rewrite

$$\begin{aligned}
\prod_{i=1}^{3}P_{q-q}(b_i) \to & F^1_{\mathrm{SP},3\mathrm{pairs}}(b_1,b_2,b_3) \\
&= \frac{\mathrm{e}^{-\frac{b^2}{2R^2_{Q\mathrm{H}}}}}{2\pi R^2_{\mathrm{H}}}\hat{P}_{q-q}(b_1)P_{q-q}(b_2)P_{q-q}(b_3) \\
&+ \frac{\mathrm{e}^{-\frac{b^2}{2R^2_{Q\mathrm{H}}}}}{2\pi R^2_{\mathrm{H}}}\hat{P}_{q-q}(b_2)P_{q-q}(b_3)P_{q-q}(b_1) \\
&+ \frac{\mathrm{e}^{-\frac{b^2}{2R^2_{Q\mathrm{H}}}}}{2\pi R^2_{\mathrm{H}}}\hat{P}_{q-q}(b_3)P_{q-q}(b_1)P_{q-q}(b_2)\,. \qquad \text{(C.2)}
\end{aligned}$$

We have the expression of the r.h.s. with (C.2) instead of $\prod_{i=1}^{3}P_{q-q}(b_i)$ in the first term of the elastic amplitude. Equation (C.1) gives the answer for the first term of the SP amplitude $\hat{A}_{3\mathrm{pairs}}(s,b)$. Of course, for obtaining $\hat{A}(s,b)_{3\mathrm{pairs}}$ we must perform such a replacement in each term of (C.1). Doing so we obtain

$$\begin{aligned}
&\hat{A}(s,b)_{3\mathrm{pairs}} \\
&= \frac{6\alpha^3}{2\pi^3}\int\prod_{i=1}^{3}\mathrm{d}^2b_i\,F^1_{\mathrm{SP},3\mathrm{pairs}}(b_1,b_2,b_3) \\
&\times \mathrm{e}^{-\frac{3\alpha}{2}(\mathbf{b}-\mathbf{b}_1/3-\mathbf{b}_2/3-\mathbf{b}_3/3)^2-\frac{\alpha}{2}(\mathbf{b}_2-\mathbf{b}_3)^2-\frac{2\alpha}{3}(\mathbf{b}_1-\mathbf{b}_2/2-\mathbf{b}_3/2)^2} \\
&+ \frac{27\alpha^3}{\pi^3}\int\prod_{i=1}^{3}\mathrm{d}^2b_i\,F^2_{\mathrm{SP},3\mathrm{pairs}}(b_1,b_2,b_3) \\
&\times \mathrm{e}^{-\frac{\alpha}{2}(3\mathbf{b}-\mathbf{b}_1-\mathbf{b}_2-\mathbf{b}_3)^2-\frac{\alpha}{2}(\mathbf{b}_2-\mathbf{b}_1)^2-\frac{3\alpha}{4}(\mathbf{b}-\mathbf{b}_3)^2} \\
&+ \frac{9\alpha^3}{\pi^3}\int\prod_{i=1}^{2}\mathrm{d}^2b_i\,F^3_{\mathrm{SP},3\mathrm{pairs}}(b_1,b_2)P_{q-q}(3b-b_2-b_1) \\
&\times \mathrm{e}^{-\frac{\alpha}{3}(3\mathbf{b}-3\mathbf{b}_1/2-3\mathbf{b}_2/2)^2-\frac{\alpha}{4}(\mathbf{b}_2-\mathbf{b}_1)^2} \\
&+ \frac{27\alpha^3}{\pi^3}\int\prod_{i=1}^{3}\mathrm{d}^2b_i\,F^4_{\mathrm{SP},3\mathrm{pairs}}(b_1,b_2,b_3) \\
&\times \mathrm{e}^{-3\alpha(\mathbf{b}-\mathbf{b}_2/2-\mathbf{b}_3/2)^2-\frac{\alpha}{2}(\mathbf{b}_2-\mathbf{b}_1)^2-\frac{\alpha}{2}(\mathbf{b}_1-\mathbf{b}_3)^2}. \qquad \text{(C.3)}
\end{aligned}$$

References

1. E. Levin, L. Frankfurt, JETP Lett. **2**, 65 (1965)
2. H.J. Lipkin, F. Scheck, Nucl. Phys. B **578**, 351 (2000)
3. A. Zamolodchikov, B. Kopeliovich, L. Lapidus, JETP Lett. **33**, 595 (1981)
4. E.M. Levin, M.G. Ryskin, Sov. J. Nucl. Phys. **45**, 150 (1987)
5. CDF Collaboration, F. Abe et al., FERMILAB-PUB-97/083-E
6. ZEUS Collaboration, J. Breitweg et al., HERA:DESY 99-160
7. A.M. Cooper-Sarkar, R.C.E. Devenish, A. De Roeck, Int. J. Mod. Phys. A **13**, 33 (1998)
8. H. Abramowicz, A. Caldwell, Rev. Mod. Phys. **71**, 1275 (1999)
9. H1 Collaboration, C. Adloff et al., Z. Phys. C **76**, 613 (1997)
10. H1 Collaboration, C. Adloff et al., Phys. Lett. B **483**, 36 (2000)
11. S. Bondarenko, E. Levin, J. Nuiri, Eur. Phys. J. C **25**, 277 (2002)
12. J.J.J. Kokkedee, The Quark Model (W.A. Benjamin, New York, 1969) and references therein
13. P.V. Landshoff, J.C. Polkinghorne, Nucl. Phys. B **133**, 541 (1971)
14. A.M. Smith et al., Phys. Lett. B **163**, 267 (1985)
15. E.K.G. Sarkisyan, A.S. Sakharov, hep-ph/0410324
16. S. Bondarenko, E. Levin, C.-I. Tan, Nucl. Phys. A **732**, 73 (2004)
17. M. Ciafaloni, M. Taiuti, A. Mueller, Nucl. Phys. B **616**, 349 (2001)

18. D.E. Kharzeev, E. Levin, Nucl. Phys. B **578**, 351 (2000)
19. D.E. Kharzeev, Y.V. Kovchegov, E. Levin, Nucl. Phys. A **690**, 621 (2001)
20. A.B. Kaidalov, Y.A. Simonov, Phys. Lett. B **477**, 163 (2000)
21. A.B. Kaidalov, Surv. High Energ. Phys. **13**, 265 (1999)
22. A. Capella, A. Kaidalov, J. Tran Thanh Van, Heavy Ion Phys. **9**, 169 (1999)
23. A. Capella, U. Sukhatme, C.I. Tan, J. Tran Thanh Van, Phys. Rep. **236**, 225 (1994)
24. O. Nachtmann, High Energy Collisions and Nonperturbative QCD, HP-THEP-96-38, hep-ph/9609365 and references therein
25. T. Shäfer, E.V. Shuryak, Rev. Mod. Phys. **70**, 323 (1998) and references therein
26. A.I. Shoshi, F.D. Steffen, H.J. Pirner, Nucl. Phys. A **709**, 131 (2002)
27. D. Kharzeev, E. Levin, K. Tuchin, Phys. Lett. B **547**, 21 (2002)
28. V.S. Fadin, L.N. Lipatov, Phys. Lett. B **429**, 127 (1998)
29. L. Motyka, Acta Phys. Pol. B **34**, 3069 (2003)
30. A. Donnachie, P.V. Landshoff, Phys. Lett. B **296**, 227 (1992)
31. A. Donnachie, P.V. Landshoff, Phys. Lett. B **437**, 408 (1998)and references therein
32. E. Levin, Everything about reggeons, DESY 97-213, hep-ph/9710546 and references therein
33. H.G. Dosch, E. Ferreira, A. Kramer, Phys. Rev. D **50**, 1992 (1994)
34. D.E. Groom et al., Eur. Phys. J. C **15** (2000)
35. J.D. Bjorken, Phys. Rev. D **47**, 101 (1993)
36. Y.L. Dokshitzer, V.A. Khoze, T. Sjöstrand, Phys. Lett. B **274**, 116 (1992)
37. E. Gotsman, E.M. Levin, U. Maor, Phys. Lett. B **309**, 199 (1993)
38. E. Gotsman, E.M. Levin, U. Maor, Phys. Lett. B **438**, 229 (1998)
39. A. Levy, Phys. Lett. B **424**, 191 (1998)
40. V. Khoze, A. Martin, M. Ryskin, Eur. Phys. J. C **18**, 167 (2000)